Hydrogeology Journal (2023) 31:621–640
https://doi.org/10.1007/s10040-023-02600-1

PAPER

Distribution of tritium-helium groundwater ages in a large Cenozoic sedimentary basin (North German Plain)

Annika Desens[1] · Georg Houben[1] · Jürgen Sültenfuß[2] · Vincent Post[3,1] · Gudrun Massmann[4]

Received: 12 May 2022 / Accepted: 19 January 2023 / Published online: 20 February 2023

Abstract

The travel time of groundwater plays a major role in the understanding of hydrogeological systems; however, large data sets necessary for regional studies of groundwater age are rare. In this study, a unique large data set of groundwater samples analysed for tritium and helium isotopes collected over the last 20 years from Cenozoic aquifers of the North German Plain is explored. Hereby, the variety of natural and technical influences on the tritium-helium age, including screen depth and length, groundwater recharge rate and climatic effects, are investigated. To a sampling depth of ~40 m below ground level, the median tritium-helium age increases almost linearly with depth, reaching a maximum of 40 years. Below, the portion of older, tritium-free water rises. The tritium-helium ages of the tritium-bearing portion increase only slightly to a maximum of about 46 years. The depth distribution of the tritium-helium age shows a dependency on groundwater recharge rates. Considering the same depth level, younger ages are related to higher groundwater recharge rates as compared to groundwater that infiltrated in areas with lower recharge rates. This is especially observed for shallow depths. Tritium-helium ages younger than 40 years are reflected well in the atmospheric tritium input curves, while deviations from it can be related to anthropogenic influences such as input from nuclear power plants and irrigation with deep, tritium-poor groundwater. The regional distribution for shallow wells indicates increasing tritium-helium ages from west to east, corresponding to decreasing groundwater recharge rates due to the more continental climate in the east.

Keywords Groundwater age · Groundwater recharge · Germany · Isotopes · Environmental tracers

Introduction

Information on the travel time of groundwater is important for the general understanding of flow processes within aquifer systems (e.g. Hinsby et al. 2001; Troldborg et al. 2008; Vandenbohede et al. 2011) as well as their vulnerability towards anthropogenic impacts such as contamination and overexploitation of groundwater resources (Böhlke and Denver 1995; Broers 2004; Hinsby et al. 2004; Houben et al. 2021). It can be helpful to obtain groundwater recharge rates (e.g. Scanlon et al. 2002; McMahon et al. 2011; Sültenfuß et al. 2011; Houben et al. 2014), to delineate protection zones (Chesnaux and Allen 2008) and to evaluate flow processes in coastal aquifers (Grünenbaum et al. 2020; Holt et al. 2021). In addition, the travel time can be used for the calibration of groundwater models (e.g. Sanford 2011; Zuber et al. 2011; Anderson et al. 2015) and for the determination of geochemical reaction rates (Seibert et al. 2019; Green et al. 2021). Travel times can be measured with (1) artificial-tracer tests, which are usually limited to maximum durations of a few months and small spatial scales, but also by (2) environmental tracers (e.g. radioactive isotopes), which are applicable for different time intervals, depending on the tracer (Cook and Böhlke 2000). For simplicity, it is assumed that conditions at the time of infiltration (e.g. temperature) are constant and the studied aquifer behaves as a steady-state system in the long term.

✉ Annika Desens
annika.desens@bgr.de

[1] Bundesanstalt für Geowissenschaften und Rohstoffe, Stilleweg 2, D-30655 Hannover, Germany

[2] Institute of Environmental Physics, University of Bremen, Otto-Hahn-Allee 1, D-28359 Bremen, Germany

[3] Edinsi Groundwater, Rivierahof 6, 1394 DC Nederhorst den Berg, Netherlands

[4] Institute of Biology and Environmental Sciences, Carl von Ossietzky University of Oldenburg, Ammerländer Heerstraße 114–118, D-26129 Oldenburg, Germany

For an ideal tracer, chemical reactions can be neglected (e.g. noble gases behave as chemically inert).

The term groundwater age, used here as a synonym for mean travel or residence time, is defined as the time elapsed between infiltration of the groundwater into the saturated zone and its sampling, and is referred to as *idealized groundwater age* (Torgersen et al. 2013), assuming flow with little impact of dispersion. When radioactive isotopes are used to determine the groundwater age, they each have a certain time range for which their application is appropriate and this age can be referred to as *tracer age* (Suckow 2014). If dispersive mixing is small, groundwater age can be used synonymously with the term tracer age. In this study, the age of young groundwater based on tritium (^{3}H) and tritiogenic helium-3 ($^3He_{trit}$) is investigated. Due to the previously mentioned conditions, the corresponding groundwater age is, therefore, referred to as *tritium-helium age*.

The determination of helium isotopes in groundwater is laborious and expensive due to the specialized sampling and analytical techniques required, and the interpretation of the data is not straightforward. The number of samples is thus limited in many studies, which restricts the focus to small study areas. Large data sets for regional studies with their inherent heterogeneity are rarely available (e.g. Broers et al. 2021; Green et al. 2021). The study presented here explores a unique, large data set of tritium-helium ages from 880 sampling locations (Fig. 1). The data were collected over the last 20 years from the Cenozoic aquifers of the North German plain, which is relatively uniform in terms of both aquifer thickness and aquifer type. The sediments are comprised predominantly of unconsolidated glacio-fluvial Quaternary and shallow marine Tertiary deposits (AD-HOC-AG Hydrogeologie 2016), which allows the region to be considered as one continuous regional aquifer body (BGR and SGD 2015). Moreover, the region is large enough to experience a gradual variation of climate, with a more humid oceanic climate in the west and a drier, more continental climate towards the east. As a result, precipitation is less frequent, but of higher intensity in the east compared to the west, and the difference between the maximum and minimum temperatures increases towards the east (Müller-Westermeier et al. 2001), which allows an in-depth assessment of the effects of regional climate variations on groundwater ages.

The objective of this study is to determine which factors and processes control the tritium-helium ages of groundwater in the North German Plain. The following aspects are addressed:

- Distribution of tritium-helium ages with depth
- Relationship between groundwater ages and groundwater recharge rates, with special emphasis on regional climatic effects
- Detection of the statistical variations of tritium-helium ages, visible only in a large data set
- Identification of borehole and sampling artefacts (e.g. screen length, leakages)
- Investigation of the limits of the tritium-helium method and of commonly used model approaches, e.g. the so-called Vogel (1970), (1967) model

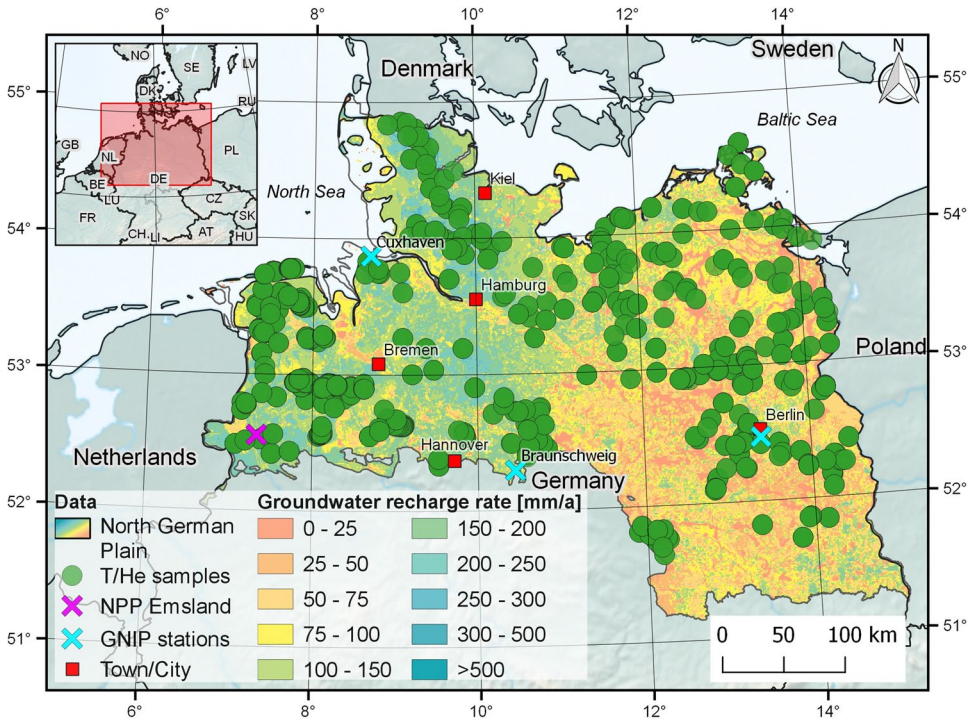

Fig. 1 Map of locations of the investigated tritium-helium (T/He) samples (data origin is described in the text and Table 1) and distribution of mean annual groundwater recharge rates (after BGR 2019) in the North German Plain. The location of the nuclear power plant (NPP) Emsland (pink cross) and the IAEA-GNIP stations Berlin, Brunswick and Cuxhaven (light blue crosses) are shown

Study area and methods

North Germany

The North German plain comprises an area of roughly 128,200 km^2 (see Fig. 1). Land use is mostly agricultural (~60 %) with some forests (~23 %). The remainders are built-up areas and nature reserves (BKG 2021a). For the latter two land use categories, groundwater age data are rare. The topographic elevation rises to 150 m above sea level (with singular peaks of up to 210 m) with an overall average elevation of around 45 m (BKG 2021b). Annual precipitation (period of 1961–1990) ranges from around 490 to 780 mm in the east and from ~570 to 1,080 mm in the west, with a median value in the east of about 622 mm and in the west of around 817 mm (DWD 2019). With rainfall rates of 280–430 mm in the east and 310–560 mm in the west, the precipitation of the summer half-year (April–September) is slightly higher than that of the winter half-year (October–March), with 190–370 mm in the east and 250–520 mm in the west (DWD 2019). Due to higher evapotranspiration in the summer (Clark and Fritz 1997), groundwater recharge takes place mainly in the winter season (Ertl et al. 2019). The river discharge is directed from the south-east to the north-west into the North Sea and the Baltic Sea.

The Cenozoic sediment cover of northern Germany contains Quaternary (Holocene as well as Pleistocene) and Tertiary deposits. The former predominantly consist of sand and gravel of glacio-fluvial origin with intercalated clay and silt layers, the latter of sandy, shallow marine deposits. The sediment cover reaches a maximum thickness of several hundred meters, whereby the layering is quasi-horizontal, except for some areas with local glaciotectonic deformations. The thickness of the Quaternary deposits ranges from 20 to 70 m, except in some subglacial channels (buried valleys) that have been eroded into the Tertiary mostly during the Elsterian glaciation, where they reach thicknesses of 350 m and more (Manhenke et al. 2001). Depending on the presence of aquitards, a vertical sequence of three to four unconsolidated porous aquifers can be distinguished. The aquitards comprise glacial tills, marls, (lacustrine) clays, silts, and lignite layers. The most important aquitard, which separates freshwater aquifers from the underlying saline aquifers and is especially widespread in large parts of north-eastern Germany (Manhenke et al. 2001) is the lower Oligocene Rupel Clay, with a thickness of up to 80 m (LBGR 2010).

Groundwater-age dating with tritium and helium-3

The radioactive hydrogen isotope tritium (half-life 12.32 a) is naturally produced in the upper layers of the atmosphere by cosmic-ray-induced spallation and fast neutron interactions with nitrogen (Craig and Lal 1961). Its concentration in water is conventionally expressed in tritium units (TU) where 1 TU corresponds to the ratio of one tritium atom to 10^{18} hydrogen atoms and equals a specific activity of 0.118 Bq/kg (Taylor and Roether 1982).

As tritium is incorporated into water molecules, it passes from the troposphere to the hydrosphere with precipitation. Due the atmospheric thermonuclear bomb tests in the late 1950s and early 1960s, the natural tritium level in the atmosphere, approximately 5 TU in precipitation of northern Europe (Roether 1967), increased up to three orders of magnitude (Clark and Fritz 1997). With groundwater recharge, tritium enters the aquifers. In the past, the estimation of groundwater travel times was done by tracking the bomb-induced peak of the highest tritium content in the unsaturated and saturated zone (Von Buttlar and Wendt 1958; Allison and Holmes 1973), which could be done by analysing tritium in vertical profiles or from time series at chosen locations.

The tritium concentration in precipitation decreased continuously after the bomb test ban treaty in 1963, due to the relatively short half-life of tritium, the continuous transport from the stratosphere to the troposphere and subsequent dilution with the ocean. In the late 1980s, routine analysis techniques for the decay product of tritium, tritiogenic helium-3, became available (Schlosser et al. 1988). The combination of tritium and tritiogenic helium-3 offers a measure for the travel time of the groundwater, which is often referred to as groundwater age. The age derived from such tracer measurements relies on the fact that the amount of tritiogenic helium-3 formed is equal to the decayed amount of tritium (assuming that no gas loss occurs) and was first described by Tolstikhin and Kamenskiy (1969). The so-called tritium-helium age is obtained from Eq. (1):

$$\tau_{trit} = \frac{1}{\lambda_{trit}} \bullet \ln\left(1 + \frac{^3He_{trit}}{^3H}\right) \quad (1)$$

where the terms are defined as follows:

τ_{trit} Tritium-helium age [in years (a)]

$^3He_{trit}$ Tritiogenic helium-3 concentration formed by β^--decay of tritium (in TU)

^3H Tritium concentration of the sample (in TU)

λ_{trit} Tritium decay constant (0.05626 a^{-1}) with half-life $t_{1/2}$ = 12.32 a (Lucas and Unterweger 2000)

Assuming that mixing and dispersion processes can be neglected, the tritium-helium age is identical to the piston-flow age. Then, the sum of tritium and the corresponding

tritiogenic helium-3 is equal to the tritium concentration in groundwater at the time of infiltration. This value is referred to as initial tritium in the following. Note that mixing of water parcels with different tritium and tritiogenic helium-3 concentrations generates a bias towards the component with the higher tracer (^3H or $^3He_{trit}$) concentration (Schlosser and Winckler 2002).

The calculation of the tritium-helium age relies on the separation of tritiogenic helium-3 from other helium-3 sources, e.g. atmospheric helium-3 ($^3He_{eq}$) and underground production (Kipfer et al. 2002). A detailed explanation of the separation procedure can be found in Kipfer et al. (2002). The assumptions and technical details for the determination of tritium-helium ages as used in this study can be found in Sültenfuß and Massmann (2004) and Sültenfuß et al. (2009).

Tritium input

Figure 2 illustrates tritium input curves in precipitation of several measuring stations, corrected for decay to January 1, 2021. The approach hence calculates the values that would have been analysed if all samples had been analysed on this day (referred to as decay-corrected tritium, $^3H_{2021}$, for details on the approach see Appendix section 'Tritium decay corrected to 2021'). Data from a recording station for tritium in precipitation in Vienna, Austria (IAEA/WMO 2021), show the longest record in Europe. In North Germany, the stations Berlin, Braunschweig (Brunswick), and Cuxhaven (for locations see Fig. 1) represent the input for the study area. Data are shown as monthly averaged values (Fig. 2a) and as a 12-month running mean (Fig. 2b). Today, tritium concentrations in precipitation are near the supposed natural value of around 5 TU. The temporal variation of the natural tritium production is related to variations in the flux of cosmic rays, due to the 11-year solar cycle (Palcsu et al. 2018). In general, tritium in precipitation is subject to influence from the atmospheric circulation and modulated by continental and seasonal effects (Cauquoin et al. 2015; Juhlke et al. 2020). As a result, higher concentrations in precipitation are found in the spring and summer months when the exchange of stratospheric air with the troposphere is increased. A continental effect can also be found: at the coast, tritium-enriched continental water vapour is diluted by tritium-depleted ocean water vapour, an effect that decreases with increasing distance from the coast (Weiss et al. 1979). In Northern Germany, this continental effect is masked by an anthropogenic feature. Tritium emissions from the French nuclear reprocessing plant at La Hague, located on the English Channel coastline, lead to significantly increased tritium concentrations in the southern North Sea water (Masson et al. 2005; BfS 2010;

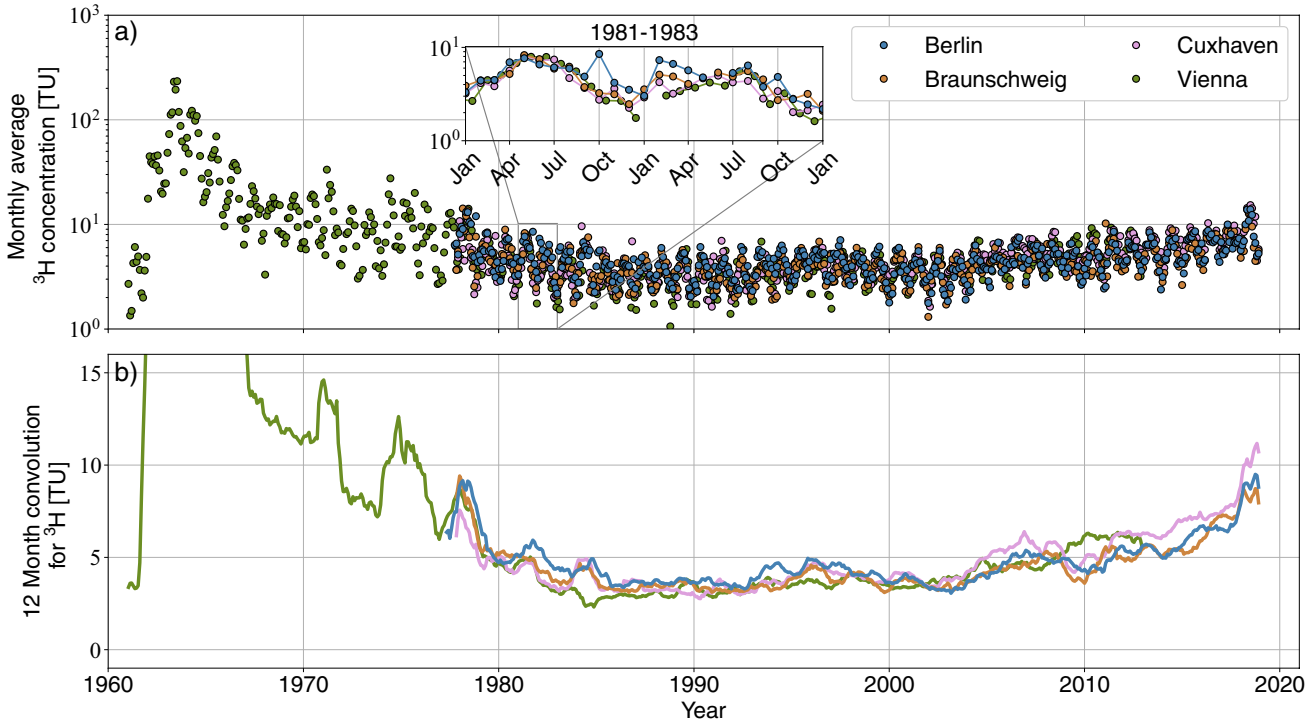

Fig. 2 Decay-corrected tritium concentrations of precipitation over time (data base: Schmidt et al. 2020; IAEA/WMO 2021): **a** Monthly average, using a logarithmic y-axis, and **b** 12-month running mean, where the y-axis is linear. The increase of the decay-corrected tritium input after 2005 (**b**) is related to the attenuation of the influence of the bomb-peak

Meyerjürgens et al. 2017). This in turn has caused a significant increase of tritium in precipitation for the coastal station Cuxhaven (Fig. 2b) since the mid-1990s. Therefore, the chosen stations represent a well-approximated average for the tritium input to groundwater.

It should be noted that decay-corrected tritium concentrations of precipitation for the period from the early 1980s to 2010 are nearly constant with values just below 5 TU (Fig. 2). This means that all recharged water during this period in Northern Germany would show the same tritium concentration in groundwater in 2021, thereby justifying that tritium concentrations in groundwater analysed within an extended time frame can be scaled to a common date, e.g. 20-year-old water analysed in 2010 exhibits the same decay-corrected tritium value as 20-year-old water analysed in 2020. This is a prerequisite to combine tritium concentration and tritium-helium ages for the data set used here, which was obtained over a period of about 20 years.

Dataset

The data set considered here contains 990 groundwater samples, which were analysed for tritium, helium isotopes and neon (Ne), collected from 880 sample locations in the period from 2001 to 2020. Some of the locations were sampled several times. All analyses were carried out at the noble gas laboratory of the Institute of Environmental Physics at the University of Bremen, Germany. The helium-3 accumulation method was used to determine the tritium concentrations (Sültenfuß et al. 2009). The samples originate from scientific publications and unpublished work commissioned by water supply companies, consulting companies or municipalities (see Table 1). A total of 106 samples with very low tritium contents (<0.1 TU), which indicate infiltration before the bomb test period, were not taken into account (see Appendix section 'Tritium in samples recharged before 1950'). In addition, 67 samples in which the analysis of tritiogenic helium-3 failed and 9 samples in which other analysis issues occurred were not considered; thus, 808 samples from 726 sampling locations were included in the investigation. All samples were analysed twice and all results of tritium and tritiogenic helium-3 were combined, resulting in up to four calculated tritium-helium ages per individual groundwater sample. In order to diminish the effect of individual outliers each age was treated as an individual data point; therefore, 2,456 calculated tritium-helium ages from the 808 samples were included in this study.

In order to enable a comparison of tritium and tritiogenic helium-3 isotope concentrations and hence tritium-helium ages in the dataset, which were analysed at different points in time, some assumptions had to be made. First, the anthropogenic influence on the aquifer dynamics was considered to be small and the flow was considered to be at steady state. Second, tritium-helium ages younger than 1 year were set to 1 year, because this is the overall precision of the method for these groundwater samples (a short explanation of this value can be found in section 'Error for tritium-helium ages').

Approximately 45% of the samples originate from production wells. In order to provide a sufficient pumping rate, the wells commonly have long screen sections (Visser et al. 2013; Cook et al. 2017) often in the length range of 10–50 m. The data set also includes a few, usually older, long-screened wells (screen length greater than 10 m). Such long screens are problematic since they can form short circuits between zones of different hydraulic heads (or temperatures), leading to significant intraborehole flow, even in the idle, nonpumping state. Since the hydrochemical composition also often varies with depth (e.g. redox zonation), the meaningfulness of samples from such wells is often compromised due to mixing (Church and Granato 1996; Puls and Paul 1997; Reilly and LeBlanc 1998; Elçi et al. 2003; Hofmann et al. 2010; Mayo 2010). The same problem arises for groundwater dating, when waters with different ages from different depths are mixed into one sample (Manning et al. 2005; Zinn and Konikow 2007; Visser et al. 2013; Jurgens et al. 2014). Samples from long screens were not excluded in the present study, opening up the opportunity to investigate the influence of the screen length on age determination.

The representativeness of water samples from production and observation wells depends strongly on their hydraulic integrity. In the ideal case, wells produce water only from the screened section, with no inflow from above or below, e.g. through leaky casing connections or faulty (or even absent) annular seals (Houben and Treskatis 2007; Horn and Harter 2009; Somaratne and Hallas 2015). In faulty wells, the inflow of young, near-surface waters in particular can compromise the age tracers of a water sample. The large data set studied here likely contains some faulty wells, although their actual percentage is unknown (Houben and Treskatis 2007). In theory, it would be possible to identify leaking wells via borehole geophysical measurements (e.g. Houben and Treskatis 2007), but this is far beyond the scope of this study. A good indicator of such damage is the presence of young groundwater, identified by tritium, krypton-85 (^{85}Kr) or anthropogenic contaminants such as pesticides, in deep wells.

Data evaluation

Groundwater samples stem from a defined depth interval, i.e. the screen length. Since the length of the well screen can play an important role in the determination of age stratification, the data were classified into different screen length classes according to Table 2. Here, the bottom depth of the well screen below ground level [mbgl] was used.

For the depth-specific box plots, the data were grouped in 3-m intervals, based on the depth of the bottom of the screen.

Table 1 Publication/data owner and number of respective samples in the data set

Data set	No. of samples
Published data sets	
Massmann et al. 2009a,b	91
Houben et al. 2014; Post et al. 2019	25
Houben et al. 2018	11
Houben et al. 2021	31
Post and Houben 2017	4
Röper et al. 2012	9
Seibert et al. 2018	17
Sültenfuß et al. 2011	40
Data owner (unpublished work)	
Gemeinde Gleichen	1
Harzwasserwerke	22
Landesamt für Bergbau, Energie und Geologie Niedersachsen	19
Landesamt für Bergbau, Geologie und Rohstoffe Brandenburg	89
Landesamt für Umwelt Brandenburg	21
Landesamt für Landwirtschaft, Umwelt und ländliche Räume Schleswig-Holstein	47
Landesamt für Umwelt, Naturschutz und Geologie Mecklenburg-Vorpommern	81
Landesbetrieb für Hochwasserschutz und Wasserwirtschaft Sachsen-Anhalt	13
Niedersächsischer Landesbetrieb für Wasserwirtschaft, Küsten- und Naturschutz	48
Oldenburgisch-Ostfriesischer Wasserverband GmbH	293
Senatsverwaltung für Umwelt, Mobilität, Verbraucher- und Klimaschutz Berlin	12
Wasserverband Lingener Land	8
Wasserverband Gifhorn GmbH	11
Zweckverband Kühlung	8
Not shown in Fig. 1	20

In the box plots, the first quartile marker represents the 25th percentile and the third quartile marker indicates the 75th percentile, while the length of the whisker corresponds to 1.5 times the interquartile range (distance between the third and the first quartile). In addition, the median values, providing there are at least five values per box, were also included.

The Vogel age for the North German Plain was calculated and compared to the measured tritium-helium age vs. depth relations. The spatial distribution of tritium-helium ages was investigated over the entire study area, considering the natural variations of climate and recharge rate. To investigate the lateral change from west to east, the tritium-helium ages and groundwater recharge rates for shallow wells were plotted and grouped into 15-km wide W–E sections (see Fig. 3b). In total, the W–E extension of about 500 km resulted in 34 such sections. For each section, box plots were produced and the respective median values were studied.

Table 2 Classification of the investigated screen lengths

Class	Description	Screen length (SL)
SL 1	Short screen	≤ 3 mbgl
SL 2	Medium screen	3 mbgl < SL < 10 mbgl
SL 3	Long screen	>10 mbgl

Groundwater recharge rate

The groundwater recharge rate exerts a strong control on the vertical groundwater age distribution, e.g. a higher recharge rate results in a faster vertical transport velocity (e.g. Houben et al. 2018). Besides the hydraulic conductivity, the groundwater recharge rate depends mostly on climatic factors such as precipitation and evapotranspiration rates (and thus on temperature), the soil type and the land cover (Müller-Westermeier et al. 2001). The commonly used model approach of Vogel (1967, 1970) assumes an age distribution over depth in an (unconfined) aquifer which depends mainly on the groundwater recharge rate, while disregarding mixing and dispersion processes. In addition, to obtain the depth-dependent frequency distribution of ages, the aquifer is assumed to have a rectangular vertical cross-section with a homogenous transmissivity

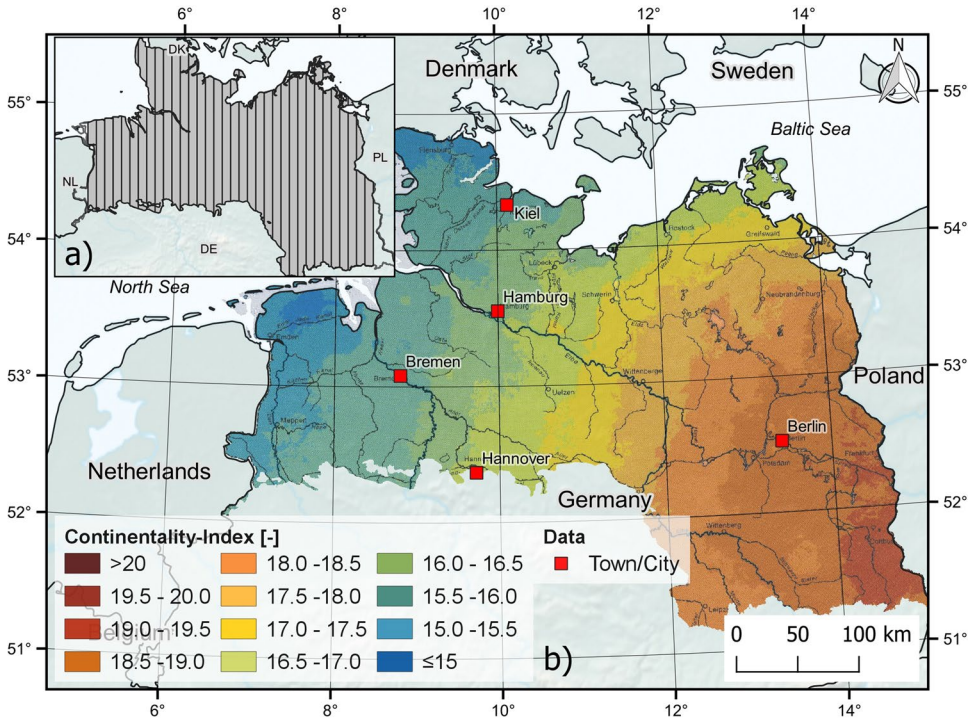

Fig. 3 **a** Distribution of the continentality index in the North German Plain (Müller-Westermeier et al. 2001) and **b** the sections for the lateral profiles of the tritium-helium age from west to east (the 34 sections have a width of 15 km each)

and porosity as well as a uniform recharge rate (Vogel 1967; Suckow 2013). In the following, this set-up will be referred to as a Vogel aquifer. For this special geometry, the groundwater age increases logarithmically with depth and is called Vogel age as expressed in Eq. (2):

$$t_{\text{Vogel}} = \frac{n \cdot H}{R} \cdot \ln\left(\frac{H}{H - z}\right) \tag{2}$$

where the terms are defined as follows:

t_{Vogel} Vogel groundwater age [T]

t_{Vogel} Effective porosity [-]

H Saturated aquifer thickness [L]

z Sample depth [L]

R Recharge rate [LT

The application of the Vogel (1967, 1970) model is justified for the aquifers studied, because they comprise relatively homogenous and horizontally deposited sandy deposits.

The average age (assuming that the age gradient between two points is linear) is then calculated as given (Cook and Böhlke 2000) in Eq. (3):

$$t_{\text{avg}} = \frac{n \cdot H}{R} \tag{3}$$

Groundwater recharge rates for the North German Plain are available at a 1 × 1 km resolution, based on a multistep regression model (Neumann 2005) for the reference period from 1961 to 1990 (BGR 2019). The annual recharge rate decreases from west to east, with median values from around 150 mm/a to approximately 75 mm/a, respectively (see Fig. 1). Parallel to the decrease of the groundwater recharge rate from west to east, the continentality index (for the years 1961 to 1990) increases in the same direction (see Fig. 3). This index determines the influence of large land masses, or likewise water masses, on the climate and the mean annual variation in temperature. Increasing continentality results in less frequent but more intense precipitation, greater temperature variations and lower annual precipitation (Müller-Westermeier et al. 2001). In addition to land use and soil properties, these parameters have a significant influence on the groundwater recharge rate. To relate tritium-helium age to recharge, each tritium-helium sample was assigned a recharge rate according to the raster map of groundwater recharge by BGR (2019). Areas of high and low recharge rates were distinguished. For this purpose, the median groundwater recharge rate of the North German Plain, which is 120 mm/a, was used as the threshold between high and low.

Results and discussion

Comparing tritium input with groundwater concentrations

Figure 4 shows the monthly averaged tritium concentrations in precipitation for the central European IAEA-GNIP stations located in the study area and in Vienna. Additionally, initial tritium (^{3}H plus ^{3}He$_{trit}$) concentrations of groundwater samples from Northern Germany for the calculated infiltration date are displayed. For groundwater sampled from wells with a short screen length, the initial tritium values closely follow the input curve from today back to about 1985. A few samples, however, deviate significantly from the input curve. This can be explained primarily by local anthropogenic influences. Samples with higher values of initial tritium originate from aquifers influenced by water from the river Ems (Sültenfuß et al. 2011, see Fig. 4 marked with "A"). Tritium from the nuclear power plant *Emsland*, in operation since 1988, is released to the river periodically. In river water samples taken directly at the outlet, the tritium concentration in the undiluted discharge reaches a maximum value of nearly 13,500 TU (BfS 2019). Due to mixing processes along the course of the river, the tritium concentration decreases, resulting in a maximum value of around 140 TU at the Ems estuary (Schmidt et al. 2020). Some of the tritium can infiltrate the adjacent aquifers following bank filtration. A similar effect is evident in groundwater samples close to the North Sea coast, due to elevated tritium concentrations in the southern North Sea (see Fig. 2). At one study site with young groundwater (marked in Fig. 4 with "B") the tritium concentration also plots below the input curve. As the screen length of the respective wells is short, a binary mixing of very old, tritium-free water with very young groundwater in the wells can be ruled out. At the site, groundwater is recharged by tritium-free, old water pumped from deeper wells used for irrigation, a common practice in NW Germany (Houben et al. 2021), causing the mixing of young and old water components.

Longitudinal dispersion in the aquifer along the flow path leads to a mixing of tracer concentrations and a more thorough inspection of the derived tracer ages is needed (Weissmann et al. 2002; Cook 2020; Massmann et al. 2009b). In the investigated data set, the distinct bomb test peak in

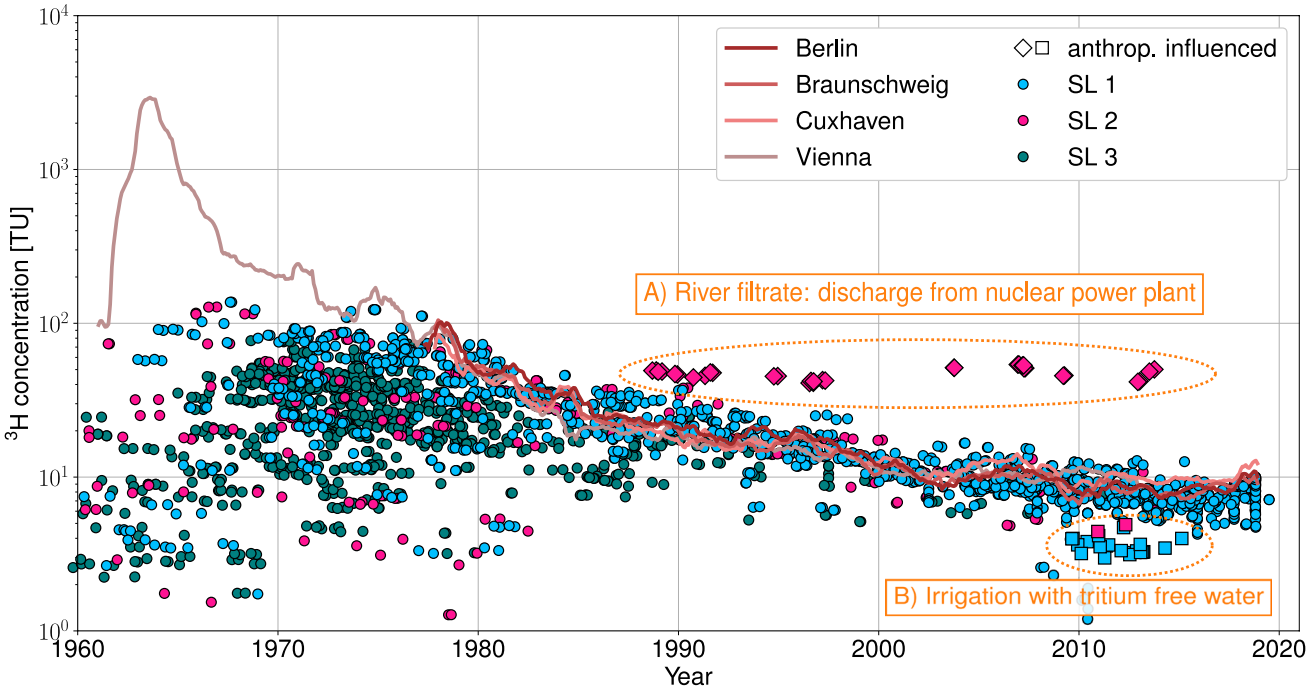

Fig. 4 Tritium in precipitation plotted as a 12-month convolution at different measuring stations in Northern Germany and Vienna, Austria (Schmidt et al. 2020; IAEA/WMO 2021) and the initial tritium concentrations at the calculated infiltration date of the dataset presented here, separated for the screen length. 'A' (marked with a diamond coloured according to the corresponding screen length class): groundwater samples in the vicinity of the nuclear power plant Emsland at the river Ems (Sültenfuß et al. 2011). 'B' (marked with a square coloured according to the corresponding screen length class): groundwater samples influenced by mixing with tritium-free irrigation water from higher depth (Houben et al. 2021)

precipitation of the 1960s is not reflected in the groundwater data, not even in samples from short screens. On the other hand, it is remarkable that initial tritium concentrations from most samples of wells with short filter screens recharged after 1985 follow the graph of tritium in precipitation, thereby implying that dispersion along the flow paths did not significantly affect the tritium-helium ages.

Wells with long or medium screen lengths are often installed at greater depths. Groundwater samples taken from such wells was thus, to a large extent, recharged before 1990. Most samples show initial tritium concentrations significantly below the tritium input concentration in the precipitation at the time of infiltration, which implies that groundwater with a calculated recharge date before 1990 must contain a tritium-free component that was recharged prior to the bomb tests (see also section 'Comparison of decay-corrected tritium with decay-corrected input curve'). This dilution with tritium-free water is probably an effect of vertical mixing within the well, induced by head and temperature gradients along the screen length and potentially also by pumping (Eberts et al. 2012; Visser et al. 2013; Jurgens et al. 2014).

Comparing the initial tritium concentration of a sample to the corresponding tritium concentration in the precipitation and calculating their ratio enables an estimation of the amount of tritium-free water in the sample. For groundwater that infiltrated before 1980, the proportion of tritium-free water amounts to 50% or more and is mostly higher in wells with longer filter screens. The portion of tritium-free water increases with increasing tritium-helium age.

Tritium-helium ages as function of depth

In Fig. 5, the tritium-helium ages and the corresponding decay-corrected tritium concentrations are shown as a function of depth for each of the three screen length classes (Table 2). The large variation in the data can be attributed to the large natural variations in climate, soil type, plant cover, aquifer type and thus recharge rates as well as technical influences (sampling, well type, etc.).

Considering the entire data set, tritium-helium ages (Fig. 5a) increase with depth as expected, but reach a limit at ~40 mbgl. Wells with a bottom screen depth of more than 40 mbgl mostly have long screens, which may be attributed to the use as water supply wells. Below 40 mbgl, the tritium-helium ages do not increase any further but scatter around 40 years. The respective groundwater samples have tritium concentrations below 3 TU (Fig. 5b), indicating that these samples contain a considerable proportion (50% or more) of tritium-free water, as discussed in section 'Influence of groundwater recharge rates on tritium-helium ages at shallow depth' (see Fig. 4). Production wells pump more or less continuously and can induce a vertical flow component causing a transport of older, tritium-free groundwater from greater depth into shallower depths.

In the shallower wells, the tritium-helium ages are more widely spread, with the majority of data stemming from observation wells with short screen lengths (SL1). Nevertheless, older groundwater can sometimes be found in shallow wells with a short screen, suggesting that the respective recharge area is far away (Sültenfuß and Massmann 2004;

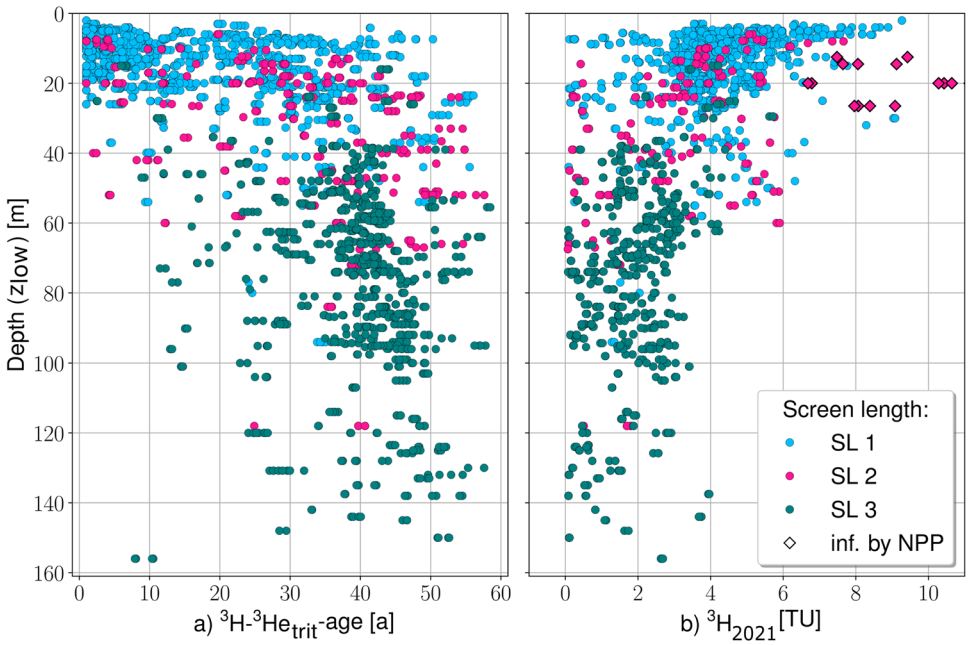

Fig. 5 **a** Tritium-helium age and **b** tritium concentration in groundwater of the North German Plain as a function of depth (defined as the bottom of the screen below ground level). The tritium concentration is decay-corrected to 2021, see section 'Tritium decay corrected to 2021'). Samples with tritium concentrations above 11 TU are not shown for overview reasons. Such high concentrations originate from samples near the river Ems and are influenced by a nuclear power plant (NPP, marked with a diamond, coloured according to the corresponding screen length class), see text

Plummer and Glynn 2013) or respective recharge rates are low, such as in swamps, clayey soils or dense forests (McMahon et al. 2011; Houben et al. 2014).

The tritium concentrations in groundwater (corrected to January 1, 2021) vs. depth is shown in Fig. 5b. Overall, the tritium concentrations decrease with depth. Samples with a tritium concentration of above 6 TU mostly originate from wells located near to the North Sea (e.g. located on the island Langeoog or in the federal state of Schleswig-Holstein) or were influenced by the discharge of a nuclear power plant (e.g. NPP Emsland). The presence of tritium at depths of up to 160 mbgl in some samples is somewhat surprising and could have been attributed to the classification, which uses the depth of the bottom of the screen rather; however, a comparison with the decay-corrected tritium concentrations plotted against the top or middle of the screen shows the same effect (see section 'Effect of bottom of screens' and the first figure therein). In addition, the tritium-helium age distribution over depth plotted at the top or middle of the screen (see section 'Effect of bottom of screens' and the second figure therein) reinforces that the occurrence of tritium at greater depth is not an artefact of using the bottom of the screen in the depth classification. Therefore, an alternative explanation could be that these wells are leaky and young water, therefore, reaches the wells through preferential flow paths in the form of leaky casing joints or in the borehole annulus due to compromised or missing annular seals. High pumping rates in wells screened at greater depths may also result in a downward transport of younger shallow groundwater (Houben et al. 2021). One example of this could be groundwater extraction from deep subglacial channels (Elbracht et al. 2016).

Figure 2b shows a minimum decay-corrected tritium concentration in precipitation for the German GNIP stations of about 3 TU, a higher value than present in most of the deep (depth > 80 mbgl) groundwater samples (see Fig. 5b). Hence, these groundwater samples must contain a tritium-free component which infiltrated prior to the bomb tests; therefore, the calculated tritium-helium age is only representative for a part of the water sample, namely its younger fraction. This underlines that individually drilled (i.e. not several screens in a single borehole) observation wells with short screen lengths in the order of 1-2 m are recommended for age dating, as they yield water samples from a defined depth interval (Houben et al. 2018).

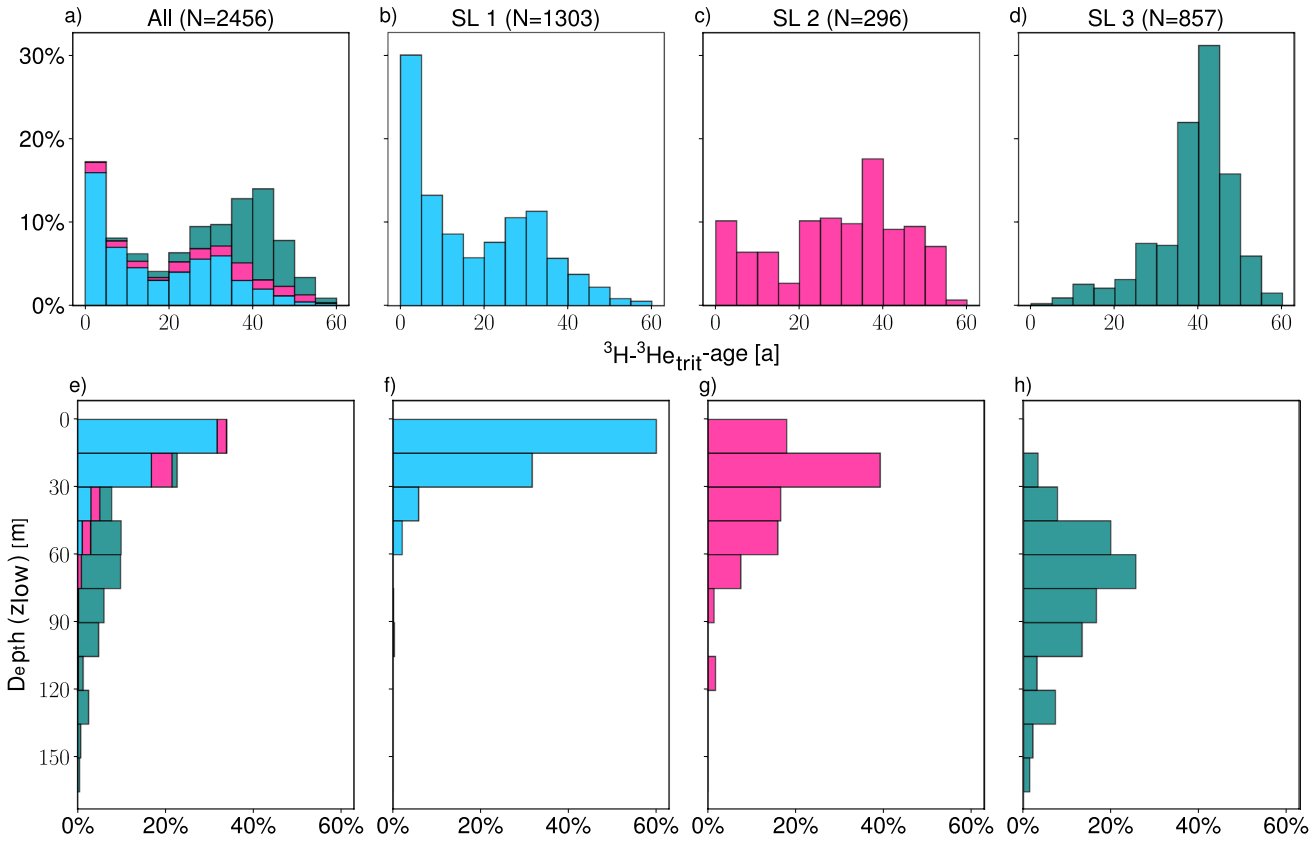

Fig. 6 Frequency distribution of the tritium-helium ages (**a**–**d**) versus the maximum filter screen depth (**e**–**h**) in the North German Plain as a function of the respective screen length. *N* indicates the number of samples considered in each case (all data, category SL1–SL3)

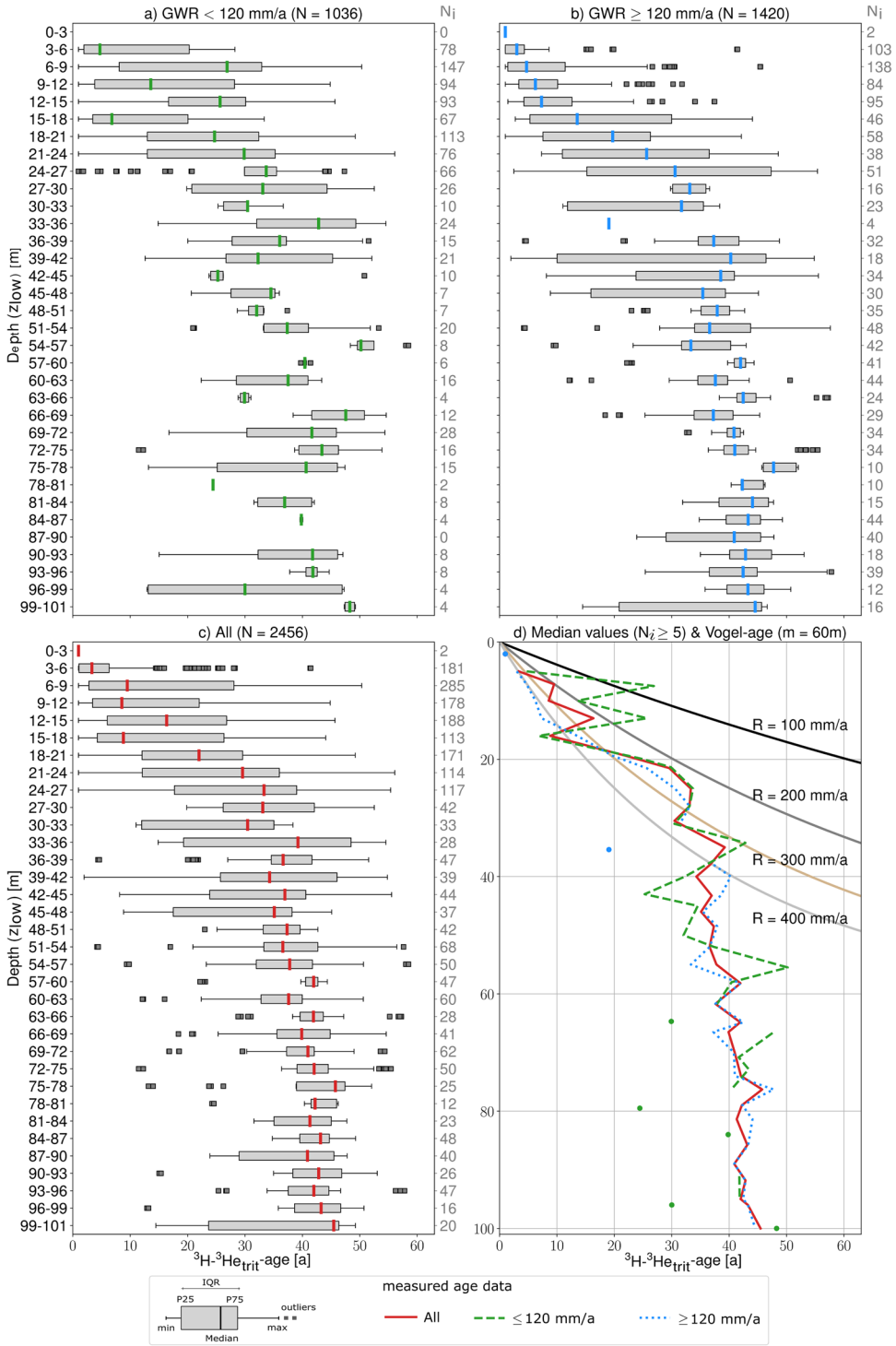

Fig. 7 Box plots of the tritium-helium age over depth, separated for the local groundwater recharge rate (GWR in mm/a). The depth is defined as the bottom of the screen below ground level. *N* describes the number of samples of each plot and N_i (on the right-hand side in grey) gives the number of samples for each box. The tritium-helium age distribution is shown for **a** recharge rates below 120 mm/a and **b** for recharge rate above 120 mm/a. **c** Illustrates the distribution for all data. The median curve (**d**) is plotted when at least five samples per box were available; otherwise, they are only plotted as single data points. **d** Shows the calculated age distributions after the Vogel model for different groundwater recharge rates and an aquifer thickness of 60 m

Figure 6a–d illustrates the corresponding frequency distribution of the tritium-helium age as a function of the screen length for the total data set (Fig. 6a) and the respective screen length classes SL 1–3 (Fig. 6b–d). The frequency distributions of the related sample depths are displayed in Fig. 6e–h. Groundwater younger than 20 years accounts for about 36% of the total data and is dominated by samples that were taken from wells with short screens (SL 1) at shallow depth (< 30 mbgl), probably stemming from observation wells. Almost 38% of the tritium-helium data indicate tritium-helium ages ranging between 20 and 40 years, with a higher proportion of samples originating from wells with long screens. Groundwater samples that fall in an age range of 40 up to 60 years represent approximately 26% of all samples. Most of these samples contain a portion of

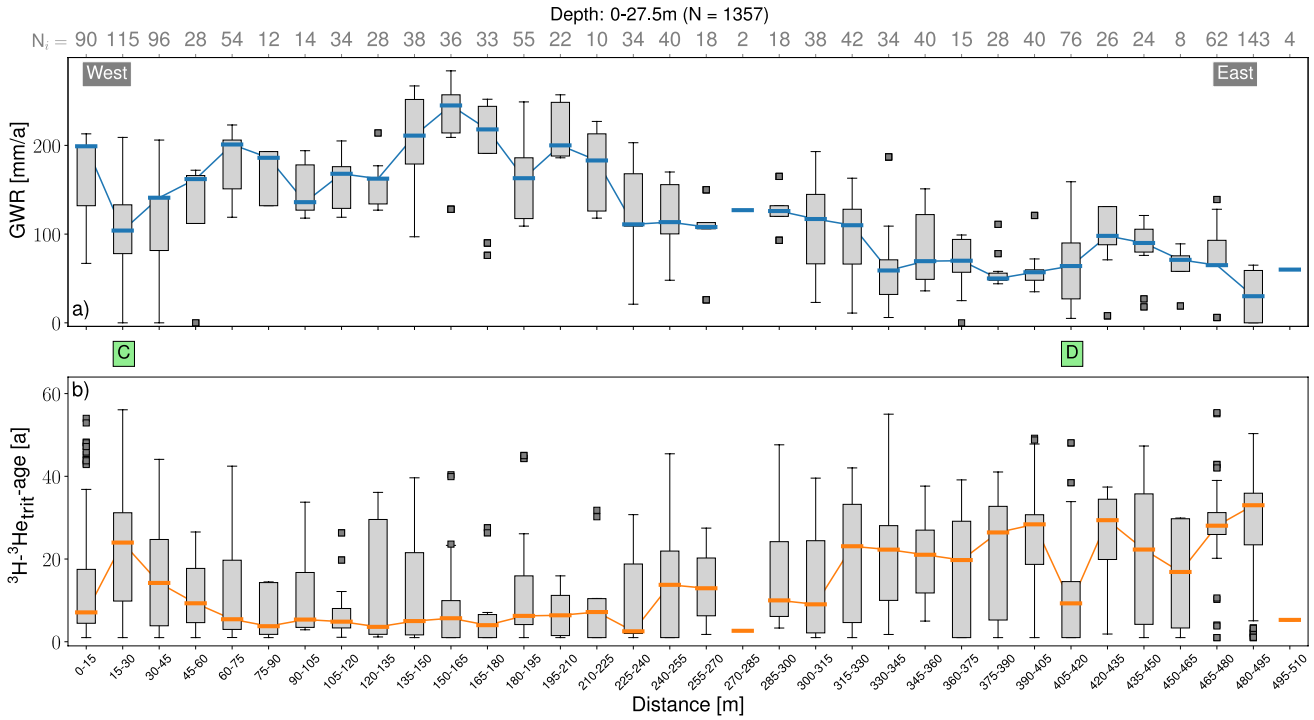

Fig. 8 Spatial distribution (west–east) of the **a** groundwater recharge rate (GWR), calculated after BGR (2019) for sections in Fig. 3 and **b** the sampled tritium-helium ages in shallow wells (bottom of the screen lower than 27.5 m) in the North German Plain. *N* describes the number of samples and N_i shows the number of samples in each box (axes above in grey). The median curve is plotted as a line if at least five samples per box are present; otherwise, they are only plotted as single data points

tritium-free water and originate predominantly from wells with long screens (SL 3) at greater depths, often production wells.

Influence of groundwater recharge rates on tritium-helium ages at shallow depth

The statistical distribution of the tritium-helium ages over depth for samples separated into classes of high and low recharge rates as well as for the complete data set is shown in Fig. 7a–c. When comparing all data (Fig. 7c), the age range, and thus the boxes, as well as the whiskers are significantly wider for shallower wells than for wells where the screen bottom is >40 mbgl. In the upper 40 mbgl, the screen lengths are mostly short (see Figs. 5 and 6), indicating that the data are well distributed vertically. The tritium-helium age trend is therefore best represented in this part of the data set. Down to a depth of around 40 mbgl, the median tritium-helium age increases almost linearly with depth, reaching a maximum of 40 years. At greater depths, the increase is much smaller, reaching a maximum tritium-helium age of 46 years (see Fig. 7d). Water sampled from deeper wells is affected by mixing with older, tritium-free groundwater, as discussed in the previous section.

When separating the data according to the groundwater recharge rates, it becomes evident that at a given depth, higher recharge rates result in younger tritium-helium ages (Fig. 7b) than do lower rates (Fig. 7a), which is consistent with the Vogel model and shows that the groundwater age is inversely proportional to the recharge rate—for unconfined aquifers, see Eqs. (2) and (3). Lower recharge rates result in lower vertical seepage velocities, while higher recharge rates lead to higher seepage velocities (Houben et al. 2014). Therefore, in this depth range, groundwater ages are strongly affected by the recharge conditions, assuming that the aquifers have similar hydraulic properties (e.g. hydraulic conductivity, porosity).

In principle, three depth zones can be defined: at shallow depths (0–15 mbgl) the tritium-helium ages are strongly affected by the recharge rate in the immediate surroundings of the well. This zone is referred to as the *site-affected zone*. This is followed by an *intermediate zone* (15–40 mbgl), where the tritium-helium ages increase almost linearly with depth, irrespective of the local recharge rates. At depths greater than 40 mbgl, the tritium-helium age variations become so small that differences caused by the groundwater recharge rate are no longer visible.

Figure 7d shows a comparison of the observed tritium-helium age distribution with the Vogel age (see Eq. 3) for different recharge rates (100–400 mm/a). For this, a relatively high aquifer thickness of 60 m was chosen, as the Vogel age is proportional to the aquifer thickness and the best fit between the tritium-helium ages and the Vogel age was achieved using this value (see section 'Vogel ages for

different aquifer thicknesses'). Overall, only the upper, almost linear part of the Vogel age-depth curve, is reflected in the observed tritium-helium ages. The latter is especially true for high recharge rates (e.g. $R = 300$ mm/a). These rates are much higher than the median recharge rates given by BGR (2019), where values from 100 to 250 mm/a are common. One explanation for this is that the BGR (2019) data set of this study also includes recharge rates from clayey soils and built-up areas and is thus shifted to some degree towards lower recharge values. For lower recharge rates ($R < 300$ mm/a), the difference between the Vogel ages and the observed tritium-helium ages is larger. If aquifer thicknesses other than 60 m are assumed, this also has an influence on the difference between the Vogel ages and the observed tritium-helium ages. Especially for thin aquifers, the deviation is large (see section 'Vogel ages for different aquifer thicknesses'). At greater depths (>40 mbgl), where the calculated tritium-helium age is only representative for a small proportion of the water sample, the tritium-helium ages observed in the North German Plain aquifers differ significantly from the Vogel age. The comparison is hampered by the fact that the Vogel model is designed for unconfined aquifers. The data set used in this study, however, includes groundwater from both confined and unconfined aquifers; therefore, when comparing tracer ages with Vogel ages, it is important to note that the comparison depends on both the application limits of the selected tracer and the aquifer geometry. In the *intermediate zone* as well as below 40 mbgl, the deviations between the Vogel age and the measured tritium-helium ages increase significantly due to the admixture of old tritium-free water.

The median tritium-helium age divided by the respective median bottom screen depth yields the average vertical propagation velocity. For the site-affected and the intermediate zone, this velocity ranges between 0.6 and 1.4 m/a, with an average value of 1.0 m/a. These values are in good agreement with vertical flow velocities previously calculated for local studies in Northern Germany (e.g. Houben et al. 2001, 2021). It should be noted that these values are of indicative value only, as they neglect local influences such as the presence of aquitards. Following the obtained average Vogel ages and using typical porosities of sandy sediments in the North German Plain ranging between 20 and 35% (Spitz and Moreno 1996), recharge rates between 120 and 490 mm/a are obtained. These values are reasonable for the context of Northern Germany, although they are somewhat higher than the median recharge rates after BGR (2019), which, however, also include clayey soils and built-up areas.

Influence of regional climate on tritium-helium ages

As the tritium-helium age is directly affected by local groundwater recharge rates only at shallow depths (especially in the site-affected zone and the intermediate zone), only tritium-helium age data from wells with a bottom of the screen < 27.5 mbgl were considered in the following. This depth value corresponds to the average depth of the intermediate zone and incidentally to an average thickness of the Quaternary in Northern Germany (often 20–30 m). The western part of Northern Germany shows a more humid oceanic climate due to its proximity to the North Sea, the prevailing westerly winds, and a drier, more continental climate towards the east. Consequently, recharge generally decreases to the east (BGR 2019; Fig. 1).

The decrease from west to east is also apparent in the median groundwater recharge rates calculated for the 15-km north–south-oriented sections (Fig. 3) in Fig. 8a. At the same time, the median tritium-helium age of the shallow groundwater increases from west to east and shows larger spread between the maximum and minimum values in the east (Fig. 8b). Hence, lower vertical seepage velocities associated with lower recharge rates are related to the increasing influence of the continental climate towards the east.

Besides some fluctuations in the tritium-helium age trend, the west–east profile shows two regions where the tritium-helium age differs from this general trend (points C and D in Fig. 8b). In the west of the North German Plain, especially at the coast, clay-rich marshes are common (BGR 2018). These marshes have low hydraulic conductivities, resulting in lower recharge rates that directly lead to comparably older tritium-helium ages at shallow depths (point C, Fig. 8). At point D, located in the east, the younger tritium-helium ages cannot be explained by higher groundwater recharge rates. Most of the data in this box originate from samples from the city of Berlin, where groundwater is recharged from surface water via bank filtration, which results in short residence times and thus young tritium-helium ages (Massmann et al. 2008; Massmann and Sültenfuß 2008).

Conclusions

The unique large tritium-helium age data set from the North German Plain allows the investigation of a variety of natural and technical influences on tracer-based groundwater age, including groundwater recharge rate, climatic effects and

screen depth and length. In addition, the benefits and the limitations of the tritium-helium method and the commonly used model approach by Vogel were assessed.

Initial tritium concentrations of groundwater obtained from short screens show good agreement with the tritium content in the precipitation at the time of infiltration. Discrepancies only occur due to anthropogenic influences, e.g. admixture of tritium-free deeper irrigation water or impacts from nuclear power plants. The bomb-test-related high tritium concentration in the precipitation in the early 1960s is not observed in the initial tritium concentration of older groundwater samples.

The investigation of the tritium-helium ages over depth shows that the median tritium-helium age increases almost linearly over the first 40 mbgl. At greater depths (>40 mbgl), the tritium-helium age scatters around a value of 40 years and does not increase much further because of mixing with older, tritium-free pre-bomb groundwater. Therefore, the tritium-helium age reflects only the young component of such groundwater samples. Such mixing is particularly pronounced in wells with long filter screens due to intra-borehole flow. For these samples, a comparison of tritium concentration in the sample with the decay-corrected input function allows one, in principle, to estimate the fraction of the older tritium-free water.

The depth distribution of the tritium-helium age shows a clear dependency on the groundwater recharge rate. For a given depth, younger ages are related to higher groundwater recharge rates, compared to older groundwater recharged with lower rates. Thereby, samples from shallow depths are strongly affected by the recharge conditions in the immediate surroundings of the well. At depths greater than 40 mbgl, the dependency of the tritium-helium age on the local groundwater recharge rate can no longer be evaluated. This is attributed to tritium concentrations reaching values below 0.1 TU.

The vertical age distribution in the aquifers of the North German Plain can mostly be described with the Vogel model. The tritium-helium age trend down to 40 mbgl follows the Vogel model quite well, especially for relatively thick aquifers (m ≥ 60 m) and higher recharge rates ($R \geq 300$ mm/a). At greater depths, the tritium-helium age differs strongly from the Vogel age due to the admixture of old groundwater, predating the atmospheric bomb tests. In contrast, a good match can be achieved at shallow depths, assuming very high recharge rates (≥300 mm/a). The regional distribution for shallow wells of the North German Plain indicates increasing tritium-helium ages from the west to the east, corresponding to decreasing groundwater recharge rates, which can be attributed to the more continental climate in the east.

Appendix

Tritium decay corrected to 2021

Scaling tritium concentrations measured in a period of 20 years: January 1, 2021 is chosen as the common date for the decay correction, as shown in Eq. (4):

$$^3H_{2021} = {}^3H(t_s) \cdot e^{-\lambda_{trit} \cdot (2021 - t_s)} \quad (4)$$

whereby the terms are defined as follows:

$^3H_{2021}$	Tritium concentration decay corrected to 2021 (in TU)
$^3H(t_s)$	Tritium concentration at the time of sampling (in TU)
t_s	Time of sampling (in a)

Error for tritium-helium ages

The overall analytical precision was assumed to be 1 year (σ_t) and is a result of analytical uncertainty of the tritium, helium isotope and neon measurements and some uncertainties for estimates of the recharge temperature and the amount of excess He in the samples.

This error of the calculated tritium-helium age (Eq. 1) can be derived from errors of tritium and tritiogenic helium-3 concentration derived with the Gaussian propagation of uncertainty. The analytical precision can be calculated as follows:

$$\sigma_{\tau_{trit}} = \sqrt{\left(\frac{\partial \tau_{trit}}{\partial {}^3He_{trit}}\right)^2 \cdot \left(\Delta {}^3He_{trit}\right)^2 + \left(\frac{\sigma_{\tau_{trit}}}{\partial {}^3H}\right)^2 \cdot \left(\Delta {}^3H\right)^2} \quad (5)$$

whereby the terms are defined as follows:

$\frac{\partial \tau_{trit}}{\partial {}^3He_{trit}}$	Partial derivative of the tritium-helium age with respect to tritiogenic helium-3 [a/TU]
$\Delta {}^3He_{trit}$	Error of tritiogenic helium-3 [TU]
$\Delta {}^3H$	Error of tritium [TU]

The partial derivatives of the tritium-helium age function (Eq. 1) results in the following equation:

$$\sigma_{\tau_{trit}} = \frac{1}{\lambda_{trit}} \cdot \frac{{}^3He_{trit}}{{}^3H + {}^3He_{trit}} \cdot \sqrt{\left(\frac{\Delta {}^3He_{trit}}{{}^3He_{trit}}\right)^2 + \left(\frac{\Delta {}^3H}{{}^3H}\right)^2} \quad (6)$$

Because the analytical error for tritium (Δ^3H) is low (0.03 TU or 3%, whatever is larger), the term $^{\Delta^3He_{trit}}/_{^3H}$ can be neglected compared to the term $^{\Delta^3He_{trit}}/_{^3He_{trit}}$. The tritogenic helium-3 could be generated with a precision of about 0.25 TU ($\Delta^3He_{trit} \leq 0.25$ TU; Sültenfuß and Massmann 2004). This error is derived from errors in sampling and analysis, as well as uncertainties in the determination of different parameters such as the excess air fraction or the infiltration temperature. For younger water with $^3H < ^3He_{trit}$ and an average tritium (^3H) concentration in the precipitation of 5 TU, the following equation applies:

$$\begin{aligned}\sigma_{\tau_{trit}} &= \frac{1}{\lambda_{trit}} \cdot \frac{^3He_{trit}}{^3H+^3He_{trit}} \cdot \sqrt{\left(\frac{\Delta^3He_{trit}}{^3He_{trit}}\right)^2 + \left(\frac{\Delta^3H}{^3H}\right)} \\ &= \frac{1}{\lambda_{trit}} \cdot \frac{^3He_{trit}}{^3H+^3He_{trit}} \cdot \frac{\Delta^3He_{trit}}{^3He_{trit}} \\ &= \frac{1}{\lambda_{trit}} \cdot \frac{\triangle^3He_{trit}}{^3H+^3He_{trit}} \\ &\approx \frac{1}{\lambda_{trit}} \cdot \frac{\triangle^3He_{trit}}{^3H} \text{ for young ages } \left(^3He_{trit} \ll ^3H\right)\end{aligned} \quad (7)$$

Using the typical values discussed previously, this would yield $\sigma_{\tau_{trit}} = \frac{12.32a}{\ln(2)} \cdot \frac{0.25TU}{5TU} \approx 0.9a \leq 1a$

Tritium in samples recharged before 1950

Even if a tritium concentration below 0.1 TU provides valuable information that the groundwater age is greater than 70 years, these data are not included, because such calculated tritium-helium ages are subject to large errors and thus are meaningless.

Groundwater that was infiltrated before the bomb tests in 1951 had an initial tritium concentration of about 5 TU, assumed for northern Europe, which after decay to today ($t = 2021$) would result in 0.1 TU $^3H(t)$. It follows that

$$^3H(t) = {}^3H\left(t_0\right) \cdot e^{-\lambda_{trit} \cdot (t-t_0)} \quad (8)$$

Using the values discussed previously would result in $^3H(t) = 5\text{ TU} \cdot e^{-\lambda_{trit} \cdot (2021-1951)} \approx 0.1\text{ TU}$

Comparison of decay-corrected tritium with decay-corrected input curve

Figure 9 compares the decay-corrected tritium input curve in precipitation and the decay-corrected tritium concentrations of groundwater samples.

Effect of bottom of screens

Figures 10 and 11 investigate the influence of using the bottom (low), the middle (mid) and the top (up) of the screen depth as sampling depth.

Vogel ages for different aquifer thicknesses

Figure 12 investigates the influence of different parameters of the Vogel (1967, 1970) model, such as recharge rate and, especially aquifer thickness. The results are compared to findings from Figure 7c, d.

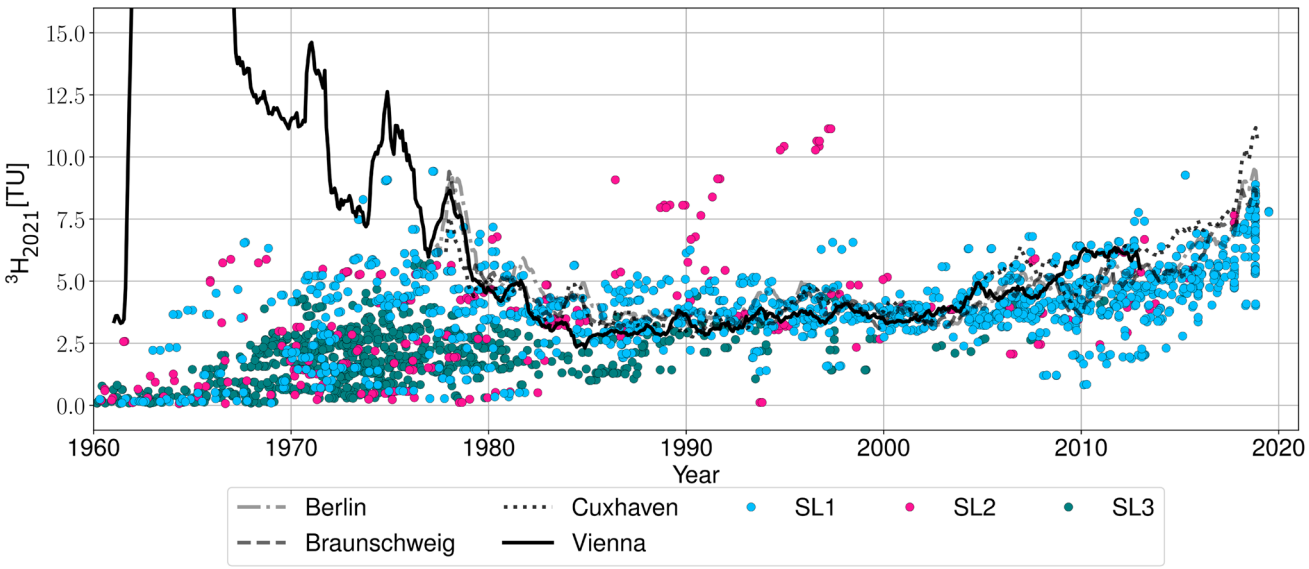

Fig. 9 Decay-corrected tritium concentrations of groundwater samples for the calculated recharge time (coloured dots) and decay-corrected tritium concentrations in precipitation (black lines)

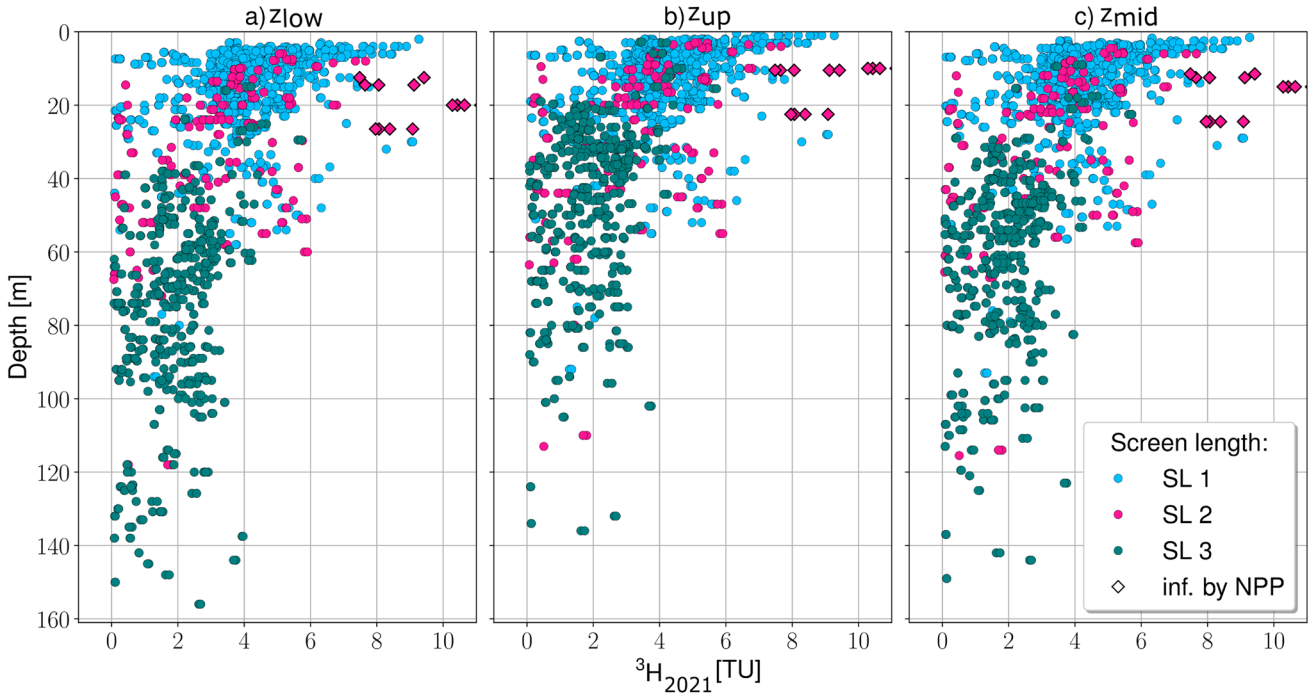

Fig. 10 Decay-corrected tritium concentration over depth as a function of screen in the North German plains. **a** The bottom of the screen, referred to as z_{low}, **b** the middle of the screen, called z_{mid} and **c** the top of the screen, referred to as z_{up}. The tritium concentration is decay-corrected to 2021. Some data at a depth of 20 m have tritium concentrations greater than 12 TU, but these are not shown here for overview reasons. Samples from river filtrates from the river Ems were influenced by a nuclear power plant (NPP) and marked with a diamond coloured according to the corresponding screen length class (SL)

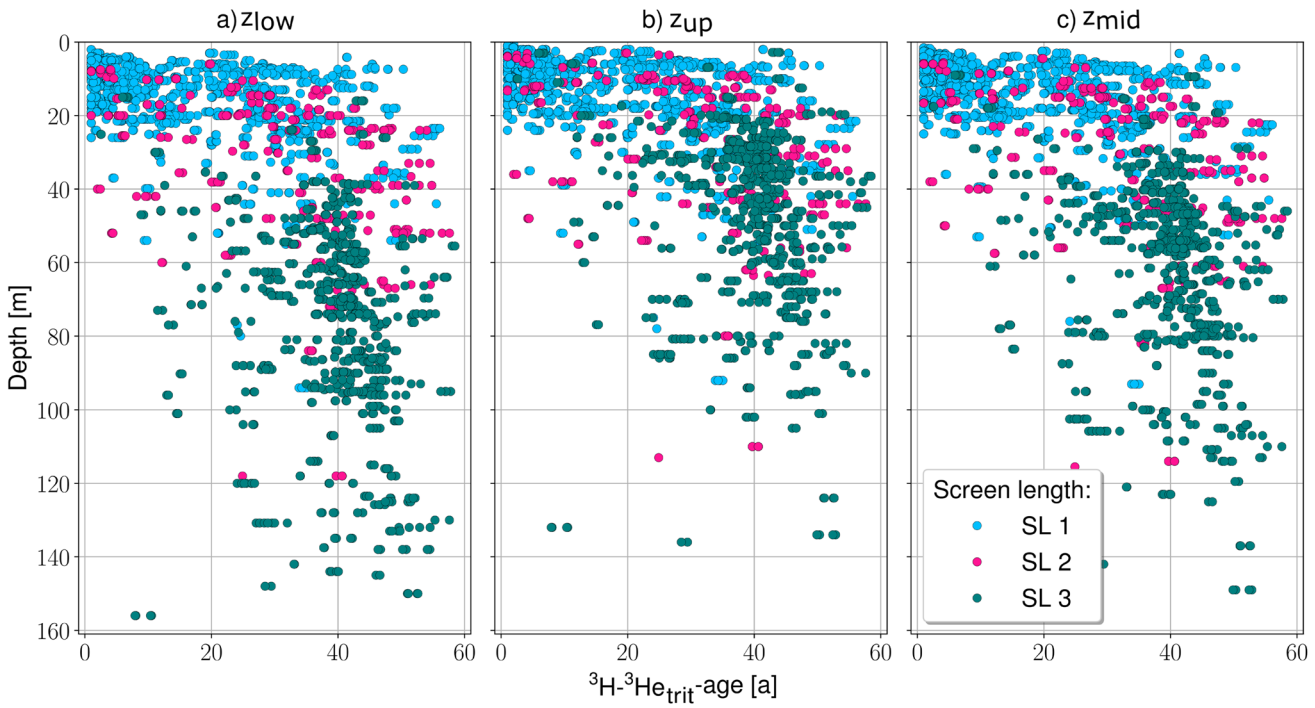

Fig. 11 Tritium-helium age over depth as a function of the screen in the North German plains. **a** The bottom of the screen, referred to as z_{low}, **b** the middle of the screen, called z_{mid}, and **c** the top of the screen, referred to as z_{up}

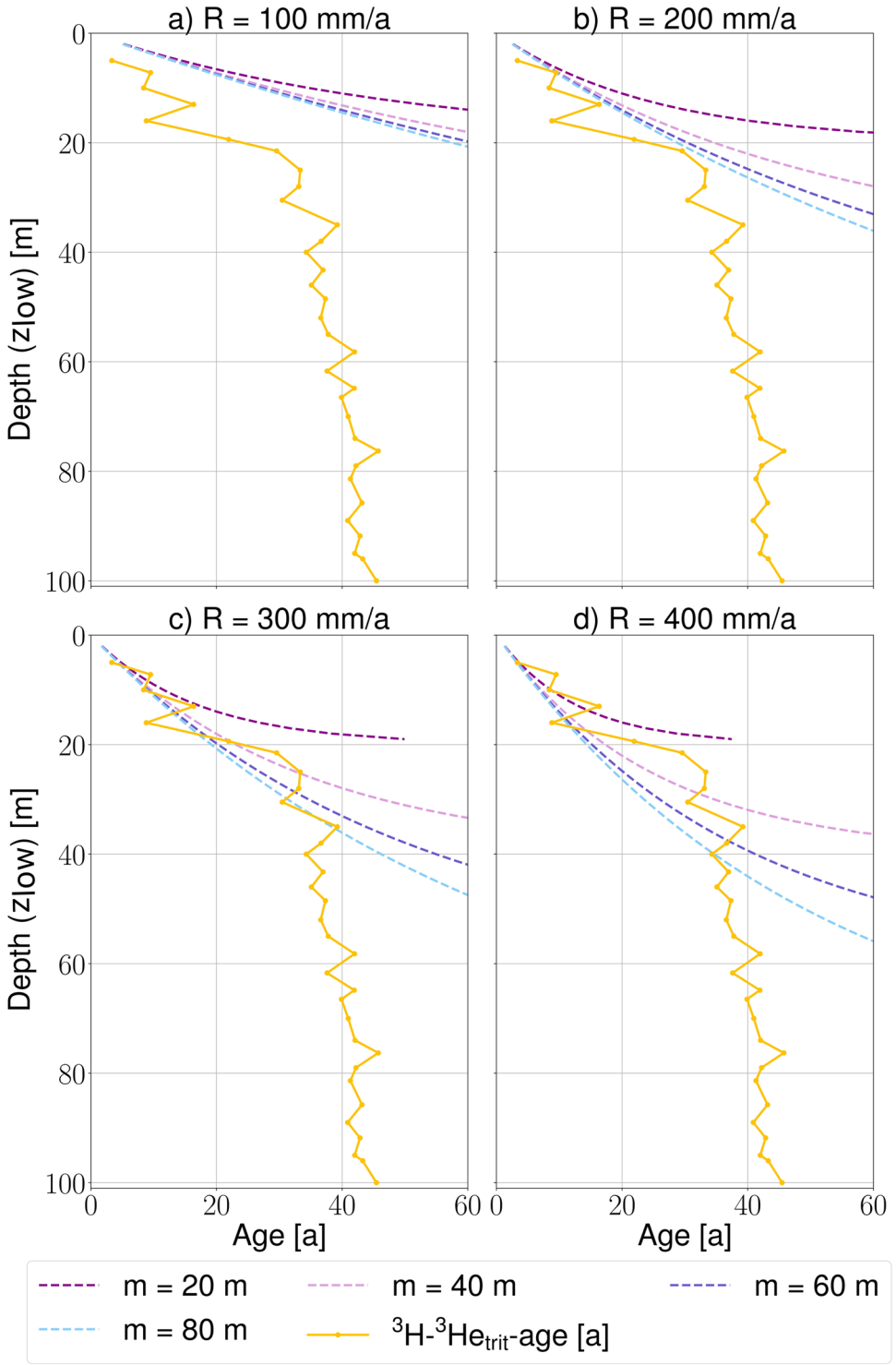

Fig. 12 **a–d** Comparison of the median tritium-helium age with the age predicted from the Vogel (1970, 1967) model. For the latter, different aquifer thicknesses (m = 20–80 m) and recharge rates (R) were assumed: **a** R = 100 mm/a, **b** R = 200 mm/a, **c** R = 300 mm/a, **d** R = 400 mm/a

Acknowledgements The authors would like to thank the many supporters involved in the compilation of the data set. These are: Ms. Zeilfelder from the SenUVK in Berlin; Mr. Brose and colleagues from the LBGR Brandenburg; Ms. Birner from the LfU Brandenburg; Mr. Barwing of the Gemeinde Gleichen; Ms. Bohn and colleagues from the LUNG MV; Ms. Budziak and Mr. Elbracht from the LBEG; Mr. de Vries and Ms. Anouchka from the NLWKN; Mr. Bach from the Landesbetrieb für Hochwasserschutz und Wasserwirtschaft Sachsen-Anhalt; Mr. Steinmann and colleagues from the LLUR SH; Geries Ingenieure GmbH, especially Ms. Böning; Mr. Führböter (BfS); Mr. Rass from the Stadtwerke Norderney; Mr. Oelrichs from the Stadtwerke Emden; Mr. Telkman, Mr. Gels and Mr. Grote (former employees) from the Wasserverband Lingener Land; Mr. Kühner from the Zweckverband Kühlung; Mr. Lehmann of the Harzwasserwerke; Mr. Schnückel from the OOWV; Mr. Raue and Ms. Fürstenberg from Enercity as well as Mr. Lampe from the WV Gifhorn and many others. In addition, the authors thank the anonymous reviewers for their constructive comments, which enhanced the quality of an earlier version of the manuscript.

Funding Open Access funding enabled and organized by Projekt DEAL.

Declarations

Conflicts of interest The authors declare no conflicting or competing interests.

References

AD-HOC-AG Hydrogeologie (2016) Regionale Hydrogeologie von Deutschland. Die Grundwasserleiter: Verbreitung, Gesteine, Lagerungsverhältnisse, Schutz und Bedeutung [Regional hydrogeology of Germany: the aquifers—distribution, rocks, tectonics, protection and importance]. Geol. Jb., A163, AG Hydrogeologie, Hannover, Germany, 456 pp

Allison GB, Holmes JW (1973) The environmental tritium concentration of underground water and its hydrological interpretation. J Hydrol 19(2):131–143. https://doi.org/10.1016/0022-1694(73)90075-9

Anderson M, Woessner W, Hunt R (2015) Applied ground water modeling: simulation of flow and advective transport. Academic, San Diego

BfS (2010) Ressortforschungsberichte zur kerntechnischen Sicherheit und zum Strahlenschutz: Kartierung von Tc-99, I-129 und I-127 im Oberflächenwasser der Nordsee – Vorhaben 3605S04481 [Federal research reports on nuclear safety and radiation protection: mapping of Tc-99, I-129 and I-127 in surface water of the North Sea - Project 3605S04481]. Bundesamt für Strahlenschutz, Berlin. http://nbn-resolving.de/urn:nbn:de:0221-201008263031. Accessed February 2023

BfS (2019) Umweltradioaktivität und Strahlenbelastung: Jahresbericht 2019 [Environmental radiation and exposure: annual report 2019]. In: Bundesamt für Strahlenschutz (BfS) and Bundesministerium für Umwelt und Naturschutz, Reaktorsicherheit und Verbraucherschutz (BMUV). http://nbn-resolving.de/urn:nbn:de:0221-2022041232235. Accessed January 2023

BGR (2018) Soil map of Germany 1:1,000,000 (BUEK1000). BGR, Hannover, Germany

BGR (2019) Mean annual groundwater recharge of Germany 1:1,000,000 (GWN1000). Digital map data v1. BGR, Hannover, Germany

BGR and SGD (2015) Hydrogeological spatial structure of Germany (HYRAUM). Digital map data v3.2. BGR, Hannover, Germany

BKG (2021a) CORINE land cover 5 ha - CLC5-2018: dl-de/by-2-0. Federal Agency for Cartography and Geodesy. https://gdz.bkg.bund.de/index.php/default/catalog/product/view/id/1071/s/corine-land-cover-5-ha-stand-2018-clc5-2018. Accessed 26 November 2021

BKG (2021b) Digitales Geländemodell Gitterweite 200 m (DGM200) [Digital terrain model grid size 200 m]. DGM1000:dl-de/by-2-0. Federal Agency for Cartography and Geodesy. https://gdz.bkg.bund.de/index.php/default/digitales-gelandemodell-gitterweite-200-m-dgm200.html. Accessed 1 March 2021

Böhlke J, Denver J (1995) Combined use of groundwater dating, chemical, and isotopic analyses to resolve the history and fate of nitrate contamination in two agricultural watersheds, Atlantic Coastal Plain, Maryland. Water Resour Res 31:2319–2339. https://doi.org/10.1029/95WR01584

Broers HP (2004) The spatial distribution of groundwater age for different geohydrological situations in the Netherlands: implications for groundwater quality monitoring at the regional scale. J Hydrol 299(1–2):84–106. https://doi.org/10.1016/j.jhydrol.2004.04.023

Broers H, Sültenfuß J, Aeschbach W, Kersting A, Menkovich A, Weert J, Castelijns J (2021) Paleoclimate signals and groundwater age distributions from 39 public water works in the Netherlands: insights from Noble gases and carbon, hydrogen and oxygen isotope tracers. Water Resour Res 57. https://doi.org/10.1029/2020WR029058

Cauquoin A, Jean-Baptiste P, Risi C, Fourré É, Stenni B, Landais A (2015) The global distribution of natural tritium in precipitation simulated with an atmospheric general circulation model and comparison with observations. Earth Planet Sci Lett 427:160–170. https://doi.org/10.1016/j.epsl.2015.06.043

Chesnaux R, Allen DM (2008) Groundwater travel times for unconfined island aquifers bounded by freshwater or seawater. Hydrogeol J 16(3):437–445. https://doi.org/10.1007/s10040-007-0241-6

Church, Granato G (1996) Bias in ground-water data caused by wellbore flow in long-screen Wells. Ground Water 34. https://doi.org/10.1111/j.1745-6584.1996.tb01886.x

Clark I, Fritz P (1997) Environmental isotopes in hydrogeology. CRC, Boca Raton, FL, 352 pp

Cook P (2020) Introduction to isotopes and environmental tracers as indicators of groundwater flow. The groundwater project. https://gw-project.org/books/introduction-to-isotopes-and-environmental-tracers-as-indicators-of-groundwater-flow/. Accessed February 2023

Cook PG, Böhlke JK (2000) Determining timescales for groundwater flow and solute transport. In: Cook PG,Herczeg AL (eds) Environmental tracers in subsurface hydrology. Springer US, Boston, MA, 30 pp. https://doi.org/10.1007/978-1-4615-4557-6_1

Cook P, Dogramaci S, McCallum J, Hedley J (2017) Groundwater age, mixing and flow rates in the vicinity of large open pit mines, Pilbara region, northwestern Australia. Hydrogeol J 25(1):39–53. https://doi.org/10.1007/s10040-016-1467-y

Craig H, Lal D (1961) The production rate of natural tritium. Tellus 13(1):86–105. https://doi.org/10.3402/tellusa.v13i1.9430

DWD (2019) Climate data center (CDC): annual regional averages of precipitation height (annual sum) in mm, version v19.3. Deutscher Wetterdienst. ttps://www.dwd.de/opendata. Accessed 21 February 2022

Eberts S, Bohlke J, Kauffman LJ, Jurgens B (2012) Comparison of particle-tracking and lumped-parameter age-distribution models

for evaluating vulnerability of production wells. Hydrogeol J 20:263–282. https://doi.org/10.1007/s10040-011-0810-6
Elbracht J, Meyer R, Reutter E (2016) Hydrogeologische Räume und Teilräume in Niedersachsen [Hydrogeological regions and subregions in Lower Saxony]. Version 17.08.2016, GeoBerichte 3 Landesamt für Bergbau, Energie und Geologie, Hanover, Germany, 118 pp. https://doi.org/10.48476/geober_3_2016
Elçi A, Flach G, Molz F (2003) Detrimental effects of natural vertical head gradients on chemical and water level measurements in observation wells: identification and control. J Hydrol 281:70–81. https://doi.org/10.1016/S0022-1694(03)00201-4
Ertl G, Bug J, Elbracht J, Engel N, Herrmann F (2019) Grundwasserneubildung von Niedersachsen und Bremen: Berechnungen mit dem Wasserhaushaltsmodell mGROWA18. Version: 17.07.2019 [Groundwater recharge in Lower Saxony and Bremen: calculations based on the water budget model mGROWA18, version 17.07.2019]. GeoBerichte 36, Landesamt für Bergbau, Energie und Geologie, Hanover, Germany, 54 pp. https://doi.org/10.48476/geober_36_2019
Green CT, Ransom KM, Nolan BT, Liao L, Harter T (2021) Machine learning predictions of mean ages of shallow well samples in the Great Lakes Basin, USA. J Hydrol 603:126908. https://doi.org/10.1016/j.jhydrol.2021.126908
Grünenbaum N, Greskowiak J, Sültenfuß J, Massmann G (2020) Groundwater flow and residence times below a meso-tidal high-energy beach: a model-based analyses of salinity patterns and 3H-3He groundwater ages. J Hydrol 587:124948. https://doi.org/10.1016/j.jhydrol.2020.124948
Hinsby K, Edmunds W, Loosli H, Manzano M, de Melo MT, Barbecot F (2001) The modern water interface: recognition, protection and development-advance of modern waters in European aquifer systems. https://doi.org/10.1144/GSL.SP.2001.189.01.16
Hinsby K, Troldborg L, Purtschert R, Corcho Alvarado J, Hofer M, Kipfer R (2004) Radionuclides (3H:85Kr) for evaluation of flow dynamics and temporal chemical trends in groundwater and surface water. Geochim Cosmochim Acta 68:A493-A493
Hofmann T, Darsow A, Gröning M, Aggarwal P, Suckow A (2010) Direct-push profiling of isotopic and hydrochemical vertical gradients. J Hydrol 385:84–94. https://doi.org/10.1016/j.jhydrol.2010.02.005
Holt T, Greskowiak J, Sültenfuss J, Massmann G (2021) Groundwater age distribution in a highly dynamic coastal aquifer. Adv Water Resour 149:103850
Horn JE, Harter T (2009) Domestic well capture zone and influence of the gravel pack length. Groundwater 47(2):277–286. https://doi.org/10.1111/j.1745-6584.2008.00521.x
Houben G, Treskatis C (2007) Water well rehabilitation and reconstruction. McGraw Hill, New York
Houben G, Martiny A, Bäßler N, Langguth HR, Plüger W (2001) Assessing the reactive transport of inorganic pollutants in groundwater of the Bourtanger moor area (NW Germany). Environ Geol 41(3):480–488. https://doi.org/10.1007/s002540100424
Houben GJ, Koeniger P, Sültenfuß J (2014) Freshwater lenses as archive of climate, groundwater recharge, and hydrochemical evolution: insights from depth-specific water isotope analysis and age determination on the island of Langeoog, Germany. Water Resour Res 50(10):8227–8239. https://doi.org/10.1002/2014wr015584
Houben GJ, Koeniger P, Schloemer S, Gröger-Trampe J, Sültenfuß J (2018) Comparison of depth-specific groundwater sampling methods and their influence on hydrochemistry, isotopy and dissolved gases: experiences from the Fuhrberger Feld, Germany. J Hydrol 557:182–196
Houben GJ, Post VEA, Gröger-Trampe J, Pesci MH, Sültenfuß J (2021) On the propagation of reaction fronts in a Sandy aquifer over 20+ years: lessons from a test site in northwestern Germany. Water Resour Res 57 (8), e2020WR028706. https://doi.org/10.1029/2020WR028706
IAEA/WMO (2021) Global Network of Isotopes in Precipitation. https://nucleus.iaea.org/wiser. Accessed January 2023
Juhlke TR, Sültenfuß J, Trachte K, Huneau F, Garel E, Santoni S, Barth JAC, van Geldern R (2020) Tritium as a hydrological tracer in Mediterranean precipitation events. Atmos Chem Phys 20(6):3555–3568. https://doi.org/10.5194/acp-20-3555-2020
Jurgens BC, Bexfield LM, Eberts SM (2014) A ternary age-mixing model to explain contaminant occurrence in a deep supply well. Ground Water 52(1):25–39. https://doi.org/10.1111/gwat.12170
Kipfer R, Aeschbach-Hertig W, Peeters F, Stute M (2002) Noble gases in lakes and ground waters. In: Donald PP, Chris JB, Rainer W (eds) Noble gases: in geochemistry and cosmochemistry. De Gruyter, Berlin, pp 615–700. https://doi.org/10.1515/9781501509056-016
LBGR (2010) Atlas zur Geologie von Brandenburg [Atlas of the geology of Brandenburg].LA f. Bergbau, Geologie und Rohstoffe, Cottbus, Germany, 157 pp
Lucas LL, Unterweger MP (2000) Comprehensive review and critical evaluation of the half-life of tritium. J Res Nat Inst Stand Technol 105(4):541–549. https://doi.org/10.6028/jres.105.043
Manhenke V, Reutter E, Hübschmann M, Limberg A, Lückstedt M, Nommensen B, Peters A, Schlimm W, Taugs R, Voigt H-J (2001) Hydrostratigraphische Gliederung des Nord- und mitteldeutschen känozoischen Lockergesteinsgebietes [Hydrostratigraphical classification of the Cenozoic unconsolidated rock regions of northern and central Germany]. Zeitchr Angewandte Geol 47:146–152 https://opus4.kobv.de/opus4-UBICO/frontdoor/index/index/docId/1385. Accessed January 2023
Manning AH, Solomon DK, Thiros SA (2005) 3H/3He age data in assessing the susceptibility of wells to contamination. Ground Water 43(3):353–367. https://doi.org/10.1111/j.1745-6584.2005.0028.x
Massmann G, Sültenfuß J (2008) Identification of processes affecting excess air formation during natural bank filtration and managed aquifer recharge. J Hydrol 359:235–246. https://doi.org/10.1016/j.jhydrol.2008.07.004
Massmann G, Sültenfuß J, Dünnbier U, Knappe A, Taute T, Pekdeger A (2008) Investigation of groundwater residence times during bank filtration in Berlin: a multi-tracer approach. Hydrol Process 22(6):788–801. https://doi.org/10.1002/hyp.6649
Massmann G, Pekdeger A, Dünnbier U, Heberer T, Richter D, Sültenfuß J, Tosaki Y (2009a) Hydrodynamische und hydrochemische Aspekte der anthropogen und natürlich induzierten Uferfiltration am Beispiel von Berlin/Brandenburg [Hydrodynamical and hydrochemical aspects of anthropogenic and naturally induced bank filtration, example Berlin/Brandenburg]. Grundwasser 14(3):163–177. https://doi.org/10.1007/s00767-009-0112-2
Massmann G, Sültenfuß J, Pekdeger A (2009b) Analysis of long-term dispersion in a river-recharged aquifer using tritium/helium data. Water Resour Res 45. https://doi.org/10.1029/2007WR006746
Masson M, Siclet F, Fournier M, Maigret A, Gontier G, Bailly du Bois P (2005) Tritium along the French coast of the English Channel. Radioprotection 40. https://doi.org/10.1051/radiopro:2005s1-091
Mayo A (2010) Ambient well-bore mixing, aquifer cross-contamination, pumping stress, and water quality from long-screened wells: what is sampled and what is not? Hydrogeol J 18:823–837. https://doi.org/10.1007/s10040-009-0568-2
McMahon PB, Plummer N, Böhlke JK, Shapiro SD, Hinkle SR (2011) A comparison of recharge rates in aquifers of the United States based on groundwater-age data. Hydrogeol J 19(4):779–800. https://doi.org/10.1007/s10040-011-0722-5
Meyerjürgens J, Badewien T, Sültenfuß J, Zielinski O (2017) Tritium as a tracer for the discrimination of water bodies in the German Bight. Geophys Res Abst 19, EGU2017-7253
Müller-Westermeier G, Kreis A, Dittmann E (2001) Klimaatlas Bundesrepublik Deutschland-Teil 2 [Climate atlas of Germany, part 2]. Deutscher Wetterdienst, Potsdam, Germany
Neumann J (2005) Flächendifferenzierte Grundwasserneubildung von Deutschland: Entwicklung und Anwendung des makroskaligen Verfahrens HAD-GWNeu [Area-specific groundwater recharge in

Germany: development and application of the macro-scale method HAD-GwNeu]. Schweizbart, Stuttgart, Germany
Palcsu L, Morgenstern U, Sültenfuss J, Koltai G, László E, Temovski M, Major Z, Nagy JT, Papp L, Varlam C, Faurescu I, Túri M, Rinyu L, Czuppon G, Bottyán E, Jull AJT (2018) Modulation of cosmogenic tritium in meteoric precipitation by the 11-year cycle of solar magnetic field activity. Sci Rep 8(1):12813. https://doi.org/10.1038/s41598-018-31208-9
Plummer LN, Glynn PD (2013) Radiocarbon dating in groundwater systems. In: Suckow A, Aggarwal PK, Araguas-Araguas L (eds) Isotope methods for dating old groundwater). IAEA, Vienna, pp 179–216
Post VEA, Houben GJ (2017) Density-driven vertical transport of saltwater through the freshwater lens on the island of Baltrum (Germany) following the 1962 storm flood. J Hydrol 551:689–702. https://doi.org/10.1016/j.jhydrol.2017.02.007
Post VEA, Houben GJ, Stoeckl L, Sültenfuß J (2019) Behaviour of tritium and Tritiogenic helium in freshwater lens groundwater systems: insights from Langeoog Island, Germany. Geofluids 2019:1–16. https://doi.org/10.1155/2019/1494326
Puls R, Paul C (1997) Multi-layer sampling in conventional monitoring wells for improved estimation of vertical contaminant distributions and mass. J Contam Hydrol 25:85–111. https://doi.org/10.1016/S0169-7722(96)00026-5
Reilly T, LeBlanc D (1998) Experimental evaluation of factors affecting temporal variability of water samples obtained from long-screened wells. Ground Water 36:566–576. https://doi.org/10.1111/j.1745-6584.1998.tb02830.x
Roether W (1967) Estimating the tritium input to groundwater from wine samples: groundwater and direct run-off contribution to central European surface waters. International Atomic Energy Agency, Vienna
Röper T, Kröger KF, Meyer H, Sültenfuss J, Greskowiak J, Massmann G (2012) Groundwater ages, recharge conditions and hydrochemical evolution of a barrier island freshwater lens (Spiekeroog, Northern Germany). J Hydrol 454–455:173–186. https://doi.org/10.1016/j.jhydrol.2012.06.011
Sanford W (2011) Calibration of models using groundwater age. Hydrogeol J 19:13–16. https://doi.org/10.1007/s10040-010-0637-6
Scanlon B, Healy R, Cook P (2002) Choosing appropriate techniques for quantifying groundwater recharge. Hydrogeol J 10:18–39. https://doi.org/10.1007/s10040-001-0176-2
Schlosser P, Winckler G (2002) Noble gases in ocean waters and sediments. In: Donald PP, Chris JB, Rainer W (eds) Noble gases: in geochemistry and cosmochemistry. De Gruyter, Stuttgart, Germany, pp 701–730. https://doi.org/10.1515/9781501509056-017
Schlosser P, Stute M, Dörr H, Sonntag C, Münnich KO (1988) Tritium/3He dating of shallow groundwater. Earth Planet Sci Lett 89(3–4):353–362. https://doi.org/10.1016/0012-821x(88)90122-7
Schmidt A, Frank G, Stichler W, Duester L, Steinkopff T, Stumpp C (2020) Overview of tritium records from precipitation and surface waters in Germany. Hydrol Process 34(6):1489–1493. https://doi.org/10.1002/hyp.13691
Seibert SL, Holt T, Reckhardt A, Ahrens J, Beck M, Pollmann T, Giani L, Waska H, Böttcher ME, Greskowiak J, Massmann G (2018) Hydrochemical evolution of a freshwater lens below a barrier island (Spiekeroog, Germany): the role of carbonate mineral reactions, cation exchange and redox processes. Appl Geochem 92:196–208. https://doi.org/10.1016/j.apgeochem.2018.03.001
Seibert SL, Greskowiak J, Prommer H, Böttcher ME, Massmann G (2019) Modeling of biogeochemical processes in a barrier island freshwater lens (Spiekeroog, Germany). J Hydrol 575:1133–1144. https://doi.org/10.1016/j.jhydrol.2019.05.094
Somaratne N, Hallas G (2015) Review of risk status of groundwater supply wells by tracing the source of coliform contamination. Water 7:3878–3905. https://doi.org/10.3390/w7073878
Spitz K, Moreno J (1996) A practical guide to groundwater and solute transport modeling. Wiley, New York
Suckow A (2013) System analysis using multitracer approaches. In: isotope methods for dating old groundwater. IAEA, Vienna, pp 217–244
Suckow A (2014) The age of groundwater: definitions, models and why we do not need this term. Appl Geochem 50:222–230. https://doi.org/10.1016/j.apgeochem.2014.04.016
Sültenfuß J, Massmann G (2004) Datierung mit der 3He-tritium-Methode am Beispiel der Uferfiltration im Oderbruch [Dating with the 3He-tritium method using the example of bank filtration in the Oderbruch]. Grundwasser 9(4):221–234
Sültenfuß J, Roether W, Rhein M (2009) The Bremen mass spectrometric facility for the measurement of helium isotopes, neon, and tritium in water. Isot Environ Health Stud 45(2):83–95. https://doi.org/10.1080/10256010902871929
Sültenfuß J, Purtschert R, Führböter J (2011) Age structure and recharge conditions of a coastal aquifer (northern Germany) investigated with ^{39}Ar, ^{14}C, ^{3}H, He isotopes and Ne. Hydrogeol J 19:221–236. https://doi.org/10.1007/s10040-010-0663-4
Taylor CB, Roether W (1982) A uniform scale for reporting low-level tritium measurements in water. Int J Appl Radiat Isotopes 33(5):377–382. https://doi.org/10.1016/0020-708X(82)90152-1
Tolstikhin IN, Kamenskiy IL (1969) About the possibility of determining the age of groundwater by using tritium-helium-3 method. Geokhimiya 8:1027–1029
Torgersen T, Purtschert R, Phillips F, Plummer LN, Sanford W, Suckow A (2013) Defining groundwater age. In: Isotope methods for dating old groundwater. IAEA, Vienna, 21–32 pp
Troldborg L, Jensen K, Engesgaard P, Refsgaard J, Hinsby K (2008) Using environmental tracers in modeling flow in a complex shallow aquifer system. J Hydrol Eng 13:1037–1048. https://doi.org/10.1061/(ASCE)1084-0699(2008)13:11(1037)
Vandenbohede A, Hinsby K, Courtens C, Lebbe L (2011) Flow and transport model of a polder area in the Belgian coastal plain: example of data integration. Hydrogeol J 19(8):1599–1615. https://doi.org/10.1007/s10040-011-0781-7
Visser A, Broers HP, Purtschert R, Sültenfuß J, De Jonge M (2013) Groundwater age distributions at a public drinking water supply well field derived from multiple age tracers (85Kr,3H/3He, and39Ar). Water Resour Res 49(11):7778–7796. https://doi.org/10.1002/2013wr014012
Vogel JC (1967) Investigation of groundwater flow with radiocarbon. International Atomic Energy Agency, Vienna
Vogel JC (1970) Carbon-14 dating of groundwater. International Atomic Energy Agency, Vienna
Von Buttlar H, Wendt I (1958) Ground-water studies in New Mexico using tritium as a tracer. Eos Trans AGU 39, 4:660–668. https://doi.org/10.1029/TR039i004p00660
Weiss W, Bullacher J, Roether W (1979) Evidence of pulsed discharges of tritium from nuclear energy installations in central European precipitation. International Atomic Energy Agency, Vienna
Weissmann GS, Zhang Y, LaBolle EM, Fogg GE (2002) Dispersion of groundwater age in an alluvial aquifer system. Water Resour Res 38(10):16-1–16-13. https://doi.org/10.1029/2001WR000907
Zinn BA, Konikow LF (2007) Potential effects of regional pumpage on groundwater age distribution. Water Resour Res 43:6. https://doi.org/10.1029/2006WR004865
Zuber A, Różański K, Kania J, Purtschert R (2011) On some methodological problems in the use of environmental tracers to estimate hydrogeologic parameters and to calibrate flow and transport models. Hydrogeol J 19(1):53–69. https://doi.org/10.1007/s10040-010-0655-4